ELSEVIER

Bone 37 (2005) 220 – 226

BONE

www.elsevier.com/locate/bone

Establishment of cementoblast cell lines from rat cementum lining cells by transfection with temperature-sensitive simian virus-40 T-antigen gene☆

Masae Kitagawa[a], Shoji Kitagawa[a], Yasusei Kudo[a], Ikuko Ogawa[c], Mutsumi Miyauchi[a], Hidetoshi Tahara[b], Toshinori Ide[b], Takashi Takata[a,c,*]

[a]*Department of Oral Maxillofacial Pathobiology, Division of Frontier Medical Science, Graduate School of Biomedical Sciences, Hiroshima University, 1-2-3 Kasumi, Minami-ku, Hiroshima 734-8553, Japan*

[b]*Department of Cell and Molecular Biology, Graduate School of Biomedical Sciences, Hiroshima University, Hiroshima 734-8553, Japan*

[c]*Center of Oral Clinical Examination, Hiroshima University Hospital, Hiroshima 734-8553, Japan*

Received 4 February 2005; revised 23 March 2005; accepted 5 April 2005
Available online 28 June 2005

Abstract

Defining the regulatory mechanisms promoting differentiation and proliferation of cementoblasts has not been well understood, because of the lack of cell models in vitro. To establish an in vitro cell model for the cementoblasts, extracted rat molars obtained from 8-week-old rats were used. Cells lining the root surface (cemetoblasts) were obtained by an enzymatic digestion method, and immediately immortalized by transfection of thermolabile SV40 T-antigen gene. The transfected cementum lining cell clones, RCM-C3 and -C4, were maintained for more than 200 population doublings (PD), while the original cells stopped their growth at 60 PD. Thus, immortalized cell lines decreased expression of SV40 T-antigen and subsequently cell proliferation at non-permissive temperature (39°C). Reverse-transcribed-polymerase chain reaction indicated expression of gene for type I collagen, alkaline phosphatase (ALP), osteopontin, and osteocalcin mRNA at both permissive (33°C) and non-permissive (39°C) temperatures. RCM-C4 expressed higher bone siaploprotein (BSP) mRNA than RCM-C3, and further RCM-C4 showed higher BSP mRNA at 39°C than 33°C. High ALP activity and mineralized nodule formation were observed at 39°C in both cell lines.

These findings suggested that the cell lines, RCM-C3 and -C4, are useful model for studying the regulatory mechanisms of differentiation and proliferation of cementoblasts.

Keywords: Cementoblast; Periodontal ligament; Immortalization; Transfection; SV40 T-antigen

Introduction

Cementum, a mineralized tissue produced by cementoblasts, covers the roots of teeth and provides for the attachment of periodontal ligament (PDL) to roots and surrounding alveolar bone [1]. There is general consensus that formation of cementum is essential for a new connective tissue attachment, subsequent to surgical treatment of periodontal disease [2–4]. However, research efforts toward understanding the regulatory mechanisms of the proliferation and differentiation of cells within the local region have been hampered by an inability to isolate and culture cementoblasts.

Recently, an immortalized cementoblast cell population from immortalized cementoblasts (OCCM), obtained from OC-TAg (OC = osteocalcin) transgenic mice has been established [5]. Although the cell line is a useful cell model for the study of cementoblast, transfected TAg may alter the cell nature of cementoblast.

In the present study, we used the plasmid pSV*ts*A58neo, encoding a thermolabile SV40 T-antigen (*ts*A58) to control effects of SV40 T-antigen [6–10], which inactivates the p53

☆ Grant support: This work was supported in part by Grants-in-Aid from the Ministry of Education, Science, and Culture of Japan.

* Corresponding author. Department of Oral Maxillofacial Pathobiology, Division of Frontier Medical Science, Graduate School of Biomedical Sciences, Hiroshima University, 1-2-3 Kasumi, Minami-ku, Hiroshima 734-8553, Japan. Fax: +81 82 257 5619.

E-mail address: ttakata@hiroshima-u.ac.jp (T. Takata).

8756-3282/$ - see front matter © 2005 Elsevier Inc. All rights reserved.
doi:10.1016/j.bone.2005.04.014

and Rb proteins [11–13]. Expression of SV40 T-antigen can be controlled by temperature, SV40 T-antigen being active at permissive temperature at 33°C and inactive non-permissive temperature at 39°C.

We previously reported a useful method to obtain a subpopulation enriched with cementoblasts from rat periodontal ligament by enzymatic digestion (*J. Dent. Res.* 2002;81:359). In the present study, to establish rat cementoblast cell lines, we transfected with temperature-sensitive SV40 T-antigen into cells of the subpopulation enriched with cementoblasts. We obtained two cell lines with characteristics of the cementoblasts, including high ALP activity, mineralized nodule formation, and expressions of mineralization-associated markers.

Materials and methods

These studies were performed in compliance with regulations administered by the experimentation committee of the Graduate School of Biomedical Sciences, Hiroshima University.

Isolation of the cementoblast-enriched cell population

According to our previously established method, we collected a subpopulation enriched with cells lining the root surface (cementoblasts) from rat PDL (*J. Dent. Res.* 2002;81:359). After sacrificing by an overdose of chloroform, molars were extracted from 10 Lewis male rats (8 weeks old, 220–250 g). To avoid contamination of experimental materials with gingival tissues, supracrestal soft tissues attached to the cervical area of the molars were carefully curettaged before extraction. The extracted molars with PDL were rinsed once in Dulbecco's phosphate-buffered saline (PBS) without calcium and magnesium (Nissui Pharmaceutical Co. Ltd., Tokyo, Japan). Next, they were immersed in a digestion solution, 20 ml of Dulbecco's Modified Eagle's Medium (DMEM, Nissui Pharmaceutical Co. Ltd.) containing 2 mg/ml collagenase (Wako, Tokyo, Japan) and 0.25% trypsin (Difco Laboratories, Detroit, MI, USA) at 37°C for 30 min. Tissues were exposed to digestion solution in 4 cycles for 20 min each and solutions were centrifuged to collect released PDL cells. We obtained 5 PDL-subpopulations (SP) by digestion of 30, 50, 70, 90, and 110 min. Using scanning electron microscopy, we have already confirmed that a few cells observed on the root surface after 90-min digestion were completely disappeared from the root surface after 110-min digestion. In addition, PDL-SP cells by 110-min digestion showed the highest activity of ALP and the largest number of mineralization nodules. Therefore, we are sure that PDL-SP by 110-min digestion is a subpopulation enriched with cells lining the root surface (cementoblasts) (data not shown).

In this study, we used the PDL-SP cells by 110-min digestion which were interpreted as a subpopulation enriched with cementoblasts. The cells were cultured in DMEM with 10% fetal bovine serum (FBS) plus penicillin G solution (10 units/ml) and streptomycin (10 mg/ml) in a humidified atmosphere of 5% CO_2 at 37°C.

Transfection with a thermolabile SV40 T-antigen gene

The pSV*ts*A58neo was kindly provided by M. Obitana (Department of Cell Biology, Institute of Development, Aging and Cancer, Tohoku University). We seeded 1×10^6 cells in 90-mm culture dishes 1 day before transfection and incubated the cells at 37°C until cells were 60%–80% confluent. Transfection was performed at 33°C with Lipofectamine Plus (Life Technologies Inc., Grand Island, NY), according to the manufacturer's protocol. Clones grown in the presence of 400 μg/ml G418 were ring-cloned, expanded, and tested for the presence of T-antigen. Cell clones were maintained in 90-mm culture dishes containing 6 ml of medium at 33°C and subcultivated at a split ratio permitting cells to be subcultured approximately once per 4 days. The split ratio varied according to the clone population doublings (PD) from 1:2 to 1:8.

Cell growth assay to assess the effect of cultural temperature

5000 cells were plated in 24-well multiwell plate with incubation for 24 h. The culture medium was then replaced with fresh medium and cells were cultured at 33°C or 39°C. Trypsinized cells were counted using a cell counter (Coulter Z1, Coulter Corp, Hialeah, Florida) at 0, 3, and 5 days.

Determination of SV40 T-antigen expression by Western blot analysis

Subconfluent cells, in 90-mm culture dishes, were used for Western blot analysis. Cells were lysed in Mammalian Protein Extraction Reagent (M-PER™; PIERCE, Rockford, IL). Protein concentration was determined by Bradford protein assay (BioRad, Laboratories, Richmond, CA) using bovine serum albumin (Sigma Chemical Co., St. Louis, MO) as a standard. 50 μg/ml of protein was solubilized in Laemmli sample buffer by boiling, and subjected to 7.5% sodium dodecylsulfate-polyacrylamide gel electrophoresis (SDS-PAGE), followed by electroblotting onto a PVDF filter treated with methanol. The filter was blocked for 1 h at 4°C with phosphate-buffered saline (PBS) buffer (137 mM NaCl, 8.1 mM $Na_2HPO_412H_2O$, 2.68 mM KCl, 1.47 mM KH_2PO_4) containing 5% nonfat dry milk powder. Western blot analysis was performed using an anti-SV40 T-antigen monoclonal antibody (Pab 101, Santa Cruz Biotechnology, Santa Cruz, CA) dissolved in PBS containing 5% nonfat dry milk powder and incubating for 60 min at room temperature. Incubation with a secondary peroxidase-coupled goat anti-mouse antibody was performed under the same conditions. For detection of the immunocomplex, an ECL

Western blotting detection system (Amersham Pharmacia Biotech., Tokyo, Japan) was used.

Measurement of ALP activity

ALP activity was assayed histochemically and biochemically. Cells were plated in 24-well multiwell plates (5×10^4 cells per well) and cultured in DMEM containing 10% FBS, penicillin G sodium (10 units/ml) and streptomycin sulfate (10 mg/ml) for 3, 6, and 9 days after confluent. Histochemical staining was performed according to a modified new fuchsin method. Briefly, after the rinse with 0.05 M Tris–HCl (pH 7.4) for 5 min at room temperature, the cells were stained with 0.05 M Tris–HCl (pH 9.8) containing 10 mg/ml of sodium naphthol AS-BI phosphate salt (Sigma-Aldrich Co., MO), 4% new fuchsin solution, and 4% sodium nitrite for 30 min. Then, the cells were fixed with 10% formaldehyde neutral buffer solution (Katayama Chemical, Tokyo, Japan) for 60 min and ALP activity was histochemically observed by light microscopy.

The quantitative analysis of ALP activity was performed biochemically by Bessey–Lowry enzymologic method using nitrophenyl phosphate as a substrate [14]. Cells were plated in 24-well multiwell plates (5×10^4 cells per well, $n = 4$) and cultured in DMEM containing 10% FBS, penicillin G sodium (10 units/ml) and streptomycin sulfate (10 mg/ml) for 5 days after confluent. The cells were washed with PBS and homogenized ultrasonically in 0.5 ml of 10 mM Tris–HCl buffer (pH 7.4) containing 25 mM $MgCl_2$. Aliquots of the homogenates were used for quantification of ALP activity.

Mineralization assay

Mineral nodule formation was detected by alizarin red S (ALZ) staining for calcium [15]. Cells were placed in a 24-well multiwell plate at a density of 5×10^4 cells per well and cultured in DMEM supplemented with 10% FBS, 50 mg/ml ascorbic acid, 10 mM sodium β-glycerophosphate, and 10 nM dexamethsone at 39°C for 3, 6, and 9 days after confluent. The cells were fixed in a 3.5% formaldehyde neutral buffer solution, and then stained with ALZ.

RNA preparation and reverse transcription-polymerase chain reaction analysis (RT-PCR)

Total RNA was isolated from cultures of confluent cells at 33°C or 39°C using the RNeasy Mini Kit (Qiagen K.K., Tokyo, Japan) according to the manufacturer's instructions. Preparations were quantified and their purity was determined by standard spectrophometric methods. cDNA was synthesized from 1 μg of total RNA according to the ReverTra Dash (Toyobo Biochemicals, Tokyo, Japan). The oligonucleotide RT-PCR primers for type I collagen (COLI), ALP, osteopontin (OPN), osteocalcin (OCN), bone sialoprotein (BSP), and glyceraldehydes-3-phosohate (GAPDH) listed in Table 1 were purchased from Invitrogen (Tokyo, Japan). Aliquots of total cDNA were amplified with 1.25 U of rTaq-DNA polymerase (Qiagen K.K.), and amplifications were performed in a PC701 thermal cycler (Astec, Fukuoka, Japan) for 30 (COLI, ALP, OPN, and OCN) and 35 (BSP) cycles after an initial 30 s denaturation at 94°C, annealed for 30 s at 56°C, and extended for 1 min at 72°C in all primers. The amplification reaction products were resolved on 1.5% agarose/TAE gels (Katayama Chemical), electrophoresed at 100 mV, and visualized by ethidium-bromide staining.

Transplantation

We transplanted cells into immunodeficient mouse. 1×10^7 cells in 100 μl of PBS were inoculated subcutaneously into 4-week-old male BALB/cAnNcrj-nu mice (Charles River Japan, Inc., Kanagawa, Japan, $n = 3$). After 3 months, we observed the transplants.

Statistical analysis

The results of cell growth analysis and quantitative ALP activity were shown as mean ± SE. According to Fisher's system, the mean values were analyzed for significance using Wilcoxon's test for non-paired examination. P values of less than 0.05 or 0.01 were judged to be statistically significant.

Results

Establishment of rat cementoblast (RCM) cell lines

Four clones (RCM-C1, -C2, -C3, -C4) were obtained by transfection with the pSV*ts*A58neo. These clones could be subcultured over 200 PD (Fig. 1A), while non-transfected original cells stopped their growth about 60 PD. We used two clones (RCM-C3 and -C4) in the following studies, because the clones showed high activities of ALP and mineralization in vitro. These cell clones showed polygonal

Table 1
Oligonucleotide primer sequences utilized in the RT-PCR

RT-PCR primer set	Sequence	Product length (bp)
COLI	F 5′-ctgaccttcctgcgcctgatgtcc-3′ R 5′-gtctggggcaccaacgtccaaggg-3′	300
ALP	F 5′-aggcaggattgaccacgg-3′ R 5-tgtagttctgctcatgga-3	440
OPN	F 5′-tccaaggagtataagcagcgggcca-3′ R 5′-ctcttagggtctaggactagcttct-3′	200
OCN	F 5′-cagccccctacccagat-3′ R 5′-gaaagtatggacggcaca-3′	232
BSP	F 5′-cactcacttgctctctccag-3′ R 5-ctgagagtgtggcgttgtgt-3	385
GAPDH	F 5′-tccaccaccctgttgctgta-3′ R 5′-accacagtccatgccatcac-3′	450

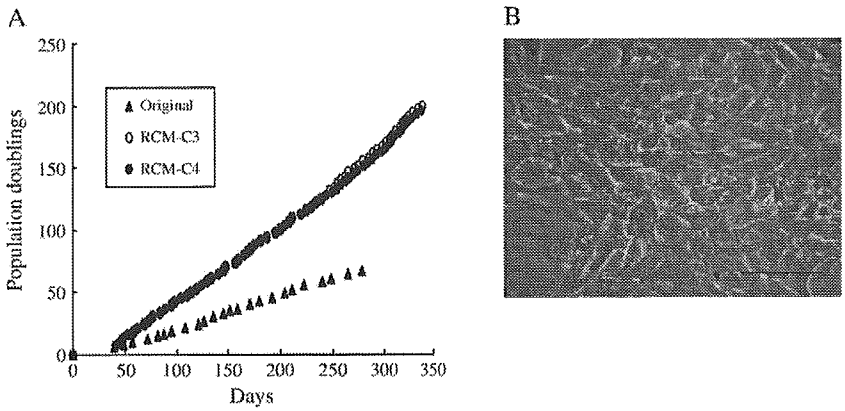

Fig. 1. (A) Population doublings (PD) of RCM cells. Original cells (Origin) stopped about 60 PD, but SV40 T-antigen-transfected clones (RCM-C3 and -C4) are immortalized and grow over 200 PD. (B) The morphology of RCM cells in culture. RCM cells were polygonal morphology and grew in monolayer (scale bar = 100 μm).

morphology in shape similar to original cells, and grew in monolayer at 39°C (Fig. 1B).

Cell proliferation of RCM cells at the permissive (33°C) or non-permissive temperatures (39°C)

Growth of the cells was significantly inhibited under the non-permissive condition, 39°C (Fig. 2A). The expression of T-antigen was decreased at 39°C compared with 33°C in both RCM cell lines (Fig. 2B).

Characterization of RCM cells

Expression of COLI, ALP, OPN, and OCN mRNA were observed in RCM-C3 and -C4 at both 33°C and 39°C (Fig. 3A). RCM-C4 expressed higher levels of BSP mRNA than RCM-C3, with greater BSP mRNA levels at 39°C vs. 33°C (Fig. 3A). Both cell lines showed higher ALP activity at 39°C than at 33°C on the 5th day (Fig. 3B). By histochemical method, both RCM-C3 and -C4 showed intense staining of ALP on the 6th day, but weak staining on the 3rd and 9th day (Figs. 3C a–c, g–i) at 39°C. RCM-C3 showed intense ALZ staining on the 6th and 9th day (Figs. 3C d–f), and RCM-C4 showed slight staining on the 6th day, and increased intensity on the 9th day (Figs. 3C j–l) at 39°C. No positive staining of ALP and ALZ was detected at 33°C in both cell lines (data not shown). Positive staining of ALZ was not observed in cells cultured in medium without supplements (50 μg/ml ascorbic acid, 10 mM β-glycerophosphate and 10 nM dexamethasone) even at 39°C (data not shown).

Transplantation of RCM cells

After 3 months, RCM cell lines transfected with SV40 T-antigen had no tumorigenesis (data not shown).

Discussion

Several efforts have been made to define the mechanism, controlling the differentiation and proliferation of cementoblasts [16–24]. However, detailed regulatory mechanisms have not yet to be completely elucidated. One of the factors hindering the detailed analyses is the lack of a stable in vitro cell model for cementoblasts.

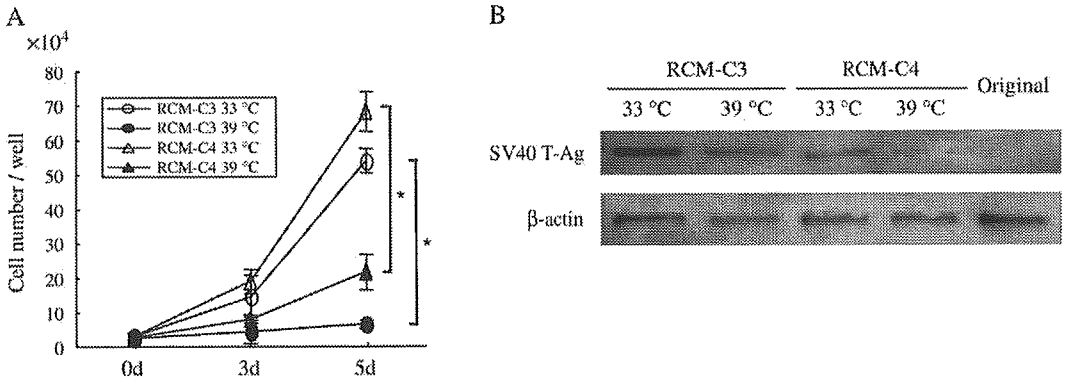

Fig. 2. (A) Growth of RCM-C3 and -C4 cells at 33°C and 39°C. *Significant difference ($P < 0.01$). (B) Expression of SV40 T-antigen in RCM-C3 and -C4 cells at 33°C and 39°C. In both cell lines, the amount of T-antigen is decreased at 39°C compared to 33°C.

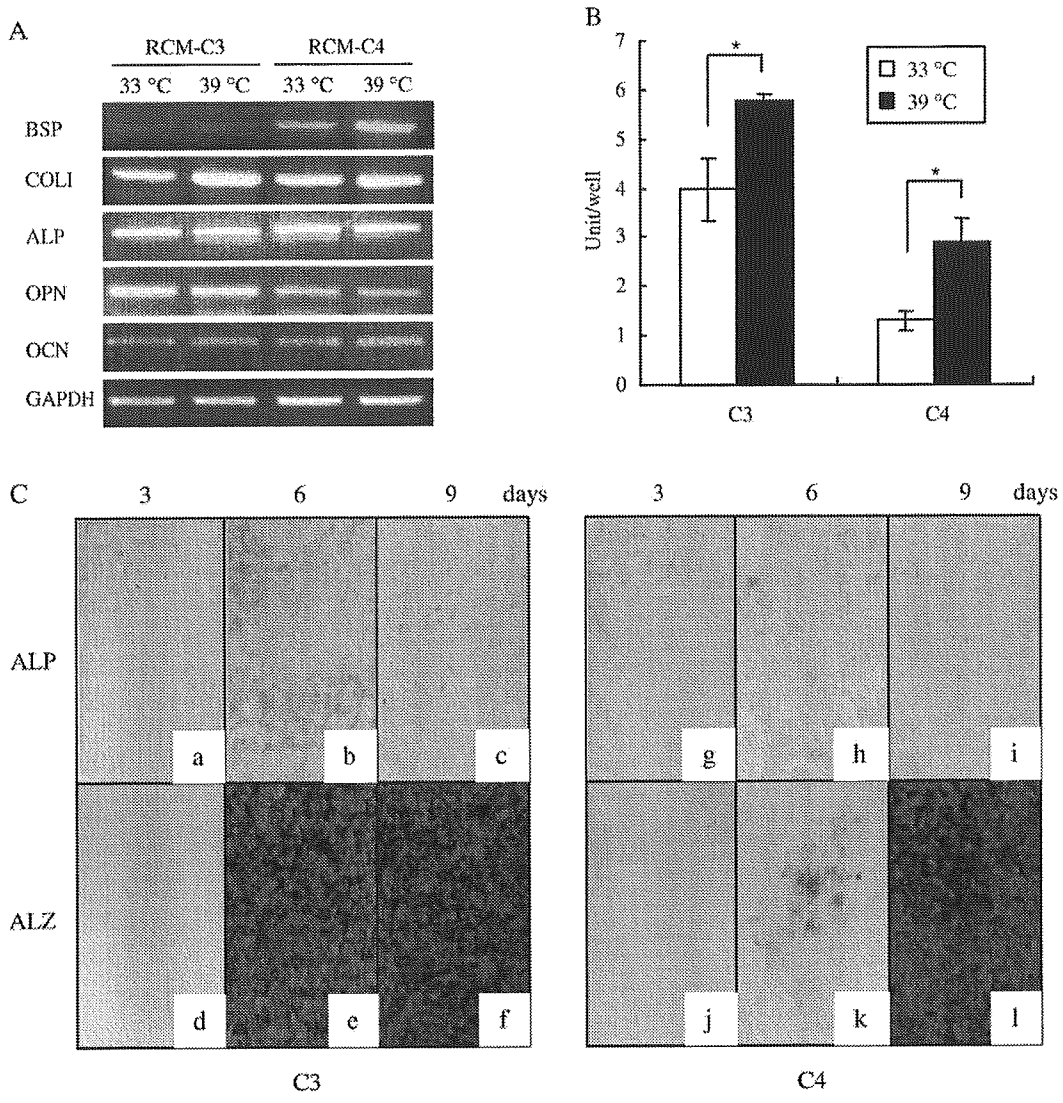

Fig. 3. (A) Gene expression of COLI, ALP, OPN, OCN, and BSP by RT-PCR in RCM-C3 and -C4 at 33°C and 39°C. (B) ALP activity by biochemical method. RCM-C3 and -C4 cells were cultured for 5 days after confluent. Both cell lines showed higher ALP activity at 39°C than 33°C. *Significant difference ($P < 0.05$). (C) ALP activity by histochemical method (a, b, c, g, h, i) and mineralization (d, e, f, j, k, l). RCM-C3 (a–f) and C4 (g–l) cells were cultured in DMEM containing 10% FBS with supplements for 3 (a, d, g, j), 6 (b, e, h, k), and 9 (c, f, i, l) days at 39°C.

In the present study, we established immortalized cementoblast cell lines, RCM-C3 and RCM-C4, by transfection with the thermolabile SV40 T-antigen into root lining cell subpopulations obtained from adult rat molars. SV40 T-antigen, which inactivates the p53 and Rb proteins, has been used to immortalize rodent and human cells [25–30]. Transfection with SV40 T-antigen results in an expanded life span for cells. The cell lines established here have continued to proliferate more 200 PD at 33°C and have not undergone senescence. The advantage of thermolabile SV40 T-antigen is to minimize the effects of transforming oncogene at the non-permissive temperature. The expression of SV40 T-antigen by RCM-C3 and -C4 disappeared at 39°C, and proliferative activity of RCM-C3 and -C4 markedly decreased. These results demonstrate that transfection of thermolabile SV40 T-antigen is effective in immortalized cells but also provide a means to examine cells under minimal effects of the antigen. Therefore, the cell line established in this study showed less effect of transformable changes, in comparison with cell lines transfected with non-thermolabile SV40 T-antigen. In addition, the shift of temperature from permissive temperature (33°C) to non-permissive temperature (39°C) induced the inhibition of proliferation and promotion of differentiation.

Cultured RCM-C3 and -C4 cells displayed the same polygonal morphology as the parent cells and grew in monolayer. Furthermore, we confirmed that RCM cell lines transfected with SV40 T-antigen had no tumorigenesis by transplantation (data not shown). This finding is consistent with the previous reports that most SV40 large T-immortalized cell lines preserve contact inhibition [31–33].

Cells immortalized with thermolabile SV40 T-antigen proliferate under permissive temperature (33°C), whereas they differentiate at non-permissive temperature (39°C). ALP activity increased at 39°C in RCM-C3 and -C4 cells. Consistent with this, RCM-C4 exhibited higher BSP mRNA levels, one of the mineralization-associated markers [34], at 39°C than 33°C.

These two cell lines expressed other mineralization-associated markers [34,35], such as COLI, ALP, OPN, and OCN mRNA, at both 33°C and 39°C by RT-PCR. These genes, shown by RT-PCR, are similar to genes reported by others to be associated with cementoblast phenotype. MacNeil et al. demonstrated that OPN, OCN, and BSP, major components of cementum, are secreted by root lining cells, cementoblasts, using immunocytochemical and in situ hybridization [36–38]. According to their study, BSP and OCN are expressed selectively in the cells lining root surface (cementoblasts) and are not expressed in PDL cells at any stage of development. In contrast, some reports that PDL cells are references to a small group of "STEM CELLS" do express OCN/BSP [39]. Nevertheless, we considered RCM-C3 and -C4 cementoblasts based on high expression of BSP or OCN as well as intense staining of ALP and ALZ by histochemical analyses. Histological staining demonstrated that the high ALP activity observed at day 6 was markedly reduced at day 9 and intense ALZ staining, suggestive of high mineralization, was observed. In support of the finding, Stain et al. reported that as osteoblast cells progress toward the mineralization stage, they exhibit measured ALP activity, histochemically, and increase mineral nodular formation, but levels of ALP mRNA decline [35].

Overall, these findings suggest that RCM-C3 and -C4 cell lines will be useful for determining mechanisms that regulate the differentiation and proliferation of cementoblasts. To examine that cell lines continue to keep the ability to produce mineral in vivo, we will try to transplant RCM cell lines in nude mice with hydroxyapatipte beads as the attachment material of cells in the future.

Acknowledgment

We are grateful to Dr. Somerman MJ for the advice and discussions during the course of this work.

References

[1] Ten Cate AR. The periodontium: oral histology: development, structure and function. Mosby: St. Louis; 2003. p. 276–9.
[2] Ten Cate AR, Mills C, Solomon G. The development of the periodontium. A transplantation and autoradiographic study. Anat Rec 1971;170:365–79.
[3] Ten Cate AR, Mills C. The development of the periodontium: the origin of alveolar bone. Anat Rec 1972;173:69–77.
[4] Ten Cate AR. Development of the periodontium. In: Cate Ten, editor. Oral histology, 4th ed. Mosby: St. Louis; 1994. p. 257–75.
[5] D'Errico JA, Ouyang H, Berry JE, MacNeil RL, Strayhorn C, Imperiale MJ, et al. Immortalized cementoblasts and periodontal ligament cells in culture. Bone 1999;25:39–47.
[6] Ide T, Tsuji Y, Nakashima T, Ishibashi S. Progress of aging in human diploid cells transformed with a tsA mutant of simirian virus 40. Exp Cell Res 1984;150:321–8.
[7] Jat PS, Noble MD, Ataliotis P, Tanaka Y, Yannoutsos N, Larsen L, et al. Direct derivation of conditionally immortal cell lines from an H-2Kb-ts58 transgenic mouse. Proc Natl Acad Sci U S A 1991;88:5096–5100.
[8] Manfredi JJ, Prives C. The transforming activity of simian virus 40 large tumor antigen. Biochim Biophys Acta 1994;1198:65–83.
[9] Tegtmeyer P. Function of simian virus 40 gene A in transforming infection. J Virol 1975;15:612–8.
[10] Yanai N, Suzuki M, Obitana M. Hepatocyte cell lines established from transgenic mice harboring temperature-sensitive simirian virus 40 large T-antigen gene. Exp Cell Res 1991;197:50–6.
[11] Eliyahu D, Raz A, Gruss P, Givol D, Oren M. Participation of p53 cellular tumour antigen in transformation of normal embryonic cells. Nature 1984;312:646–9.
[12] Jenkins JR, Rudge K, Currie GA. Cellular immortalization by a cDNA clone encoding the transformation-associated phosphoprotein p53. Nature 1984;312:651–4.
[13] Rassoulzadegan M, Cowie A, Carr A, Glaichenhaus N, Kamen R, Cuzin F. The roles of individual polyoma virus early proteins in oncogenic transformation. Nature 1982;300:713–8.
[14] Bessey OA, Lowry OH, Brock MJ. A method for the rapid detemination of alkaline phosphatase with five cubic millimeter of serum. J Biol Chem 1946;164:321–9.
[15] Dahl LK. A simple and sensitive histochemical method for calcium. Proc Soc Exp Biol Med 1952;80:474–9.
[16] Bosshardt DD, Zalzal S, McKee MD, Nanci A. A developmental appearance and ditribution of bone sialoprotein and osteopontin in human and rat cementum. Anat Rec 1998;250:13–33.
[17] D'Errico JA, Berry JE, Ouyang H, Strayhorn C, Windle JJ, Somerman MJ. Employing a transgenic animal model to obtain cementoblasts, in vitro. J Periodontol 2000;71:63–72.
[18] Grzesik WJ, Kuznetsov SA, Uzawa K, Mankani M, Gehron Robey P, Yamauchi M. Normal human cementum-derived cells: isolation, clonal expansion, and in vitro and in vivo characterization. J Bone Miner Res 1998;13:547–1554.
[19] MacNeil RL, D'Errico JA, Ouyang H, Berry J, Strayhorn C, Somerman MJ. Isolation of murine cementoblasts: unique cells or uniquely-positioned osteoblasts? Eur J Oral Sci 1998;106(Suppl I):350–6.
[20] Nohutcu RM, McCauley LK, Koh AJ, Somerman MJ. Expression of extracellular matrix proteins in human periodontal ligament cells during mineralization in vitro. J Periodontol 1997;68:320–7.
[21] Ouyang H, McCauley LK, Berry JE, D'Errico JA, Strayhorn CL, Somerman MJ. Response of immortalized murine cementoblasts/periodontal ligament cells to parathyroid hormone and parathyroid hormone-related protein in vitro. Arch Oral Biol 2000;45:293–303.
[22] Ouyang H, McCauley LK, Berry JE, Saygin NE, Tokiyasu Y, Somerman MJ. Parathyroid hormone-related protein regulates extracellular matrix gene expression in cementoblasts and inhibits cementoblast-mediated mineralization in vitro. J Bone Miner Res 2000;15:2140–2153.
[23] Ramakrishnan PR, Lin WL, Sodek J, Cho MI. Synthesis of non-collagenous extracellular matrix proteins during development of mineralized nodules by rat periodontal ligament cells in vitro. Calcif Tissue Int 1995;57:52–9.
[24] Saygin N, Giannobile WV, Somerman MJ. Molecular and cell biology of cementum. Periodontology 2000;24:73–98.

[25] Jat PS, Sharp PA. Large T antigens of simian virus 40 and polyomavirus efficiently establish primary fibroblasts. J Virol 1986;59:746–50.
[26] Petit CA, Gardes M, Feunteun J. Immortalization of rodent embryo fibroblasts by SV40 is maintained by the A gene. Virology 1983;127: 74–82.
[27] Powell AJ, Darmon AJ, Gonos ES, Lam EW, Peden KW, Jat PS. Different functions are required for initiation and maintenance of immortalization of rat embryo fibroblasts by SV40 large T antigen. Oncogene 1999;18:7343–50.
[28] Shay JW, Van Der Haegen BA, Ying Y, Wright WE. The frequency of immortalization of human fibroblasts and mammary epithelial cells transfected with SV40 large T-antigen. Exp Cell Res 1993;209:45–52.
[29] Todaro GJ, Green H. Quantitative studies of the growth of mouse embryo cells in culture and their development into established lines. J Cell Biol 1963;17:299–313.
[30] Yanai N, Satoh T, Kyo S, Abe K, Suzuki M, Obitana M. A tubule cell line established from transgenic mice harboring temperature-sensitive simirian virus 40 large T-antigen gene. Jpn J Cancer Res 1991;82: 1344–1348.
[31] Meek RL, Bowman PD, Daniel CW. Establishment of mouse embryo cells in vitro. Relationship of DNA synthesis, senescence and malignant transformation. Exp Cell Res 1977;107:277–84.
[32] Wieser RJ, Faust D, Dietrich C, Oesch F. p16INL4a mediates contact inhibition of growth. Oncogene 1999;18:228–77.
[33] Zhang HS, Postigo AA, Dean DC. Active transcriptional repression by the Rb-E2F complex mediates G1 arrest triggered by p16INK4a, TGF-β, and contact inhibition. Cell 1999;97:53–61.
[34] Aubin JE, Liu F, Malaval L, Gupta AK. Osteoblast and chondroblast differentiation. Bone 1995;17:77S–83S [Suppl].
[35] Stain GS, Lian JB. Molecular mechanisms mediation proliferation/ differentiation interrelationships during progressive development of osteoblast phenotype. Endocr Rev 1993;14:424–42.
[36] D'Errico JA, MacNeil RL, Takata T, Berry J, Strayhorn C, Somerman MJ. Expression of bone associated markers by tooth root lining cells, in situ and in vitro. Bone 1997;20:117–26.
[37] MacNeil RL, Sheng N, Strayhorn C, Fishier LW, Somerman MJ. Bone sialoprotein is localized to the root surface during cementogenesis. J Bone Miner Res 1994;9:1597–606.
[38] Macneil RL, Berry J, Strayhorn C, Somerman MJ. Expression of bone sialoprotein mRNA by cells lining the mouse tooth root during cementogenesis. Arch Oral Biol 1996;41:827–35.
[39] Berry JE, Zhao M, Jin Q, Foster BL, Viswanathan H, Somerman MJ. Exploring the origin of cementoblasts and trigger factors. Connect Tissue Res 2003;44:97–102.

ELSEVIER

Bone 38 (2006) 420–426

BONE

www.elsevier.com/locate/bone

Characteristics of periodontal ligament subpopulations obtained by sequential enzymatic digestion of rat molar periodontal ligament

T. Kaneda [a,b], M. Miyauchi [a], T. Takekoshi [a], S. Kitagawa [a], M. Kitagawa [a], H. Shiba [b], H. Kurihara [b], T. Takata [a,*]

[a] *Department of Oral Maxillofacial Pathobiology, Division of Frontier Medical Science, Graduate School of Biomedical Sciences, Hiroshima University, 1-2-3 Kasumi, Minami-ku, Hiroshima 734-8553, Japan*

[b] *Department of Periodontal Medicine, Division of Frontier Medical Science, Graduate School of Biomedical Sciences, Hiroshima University, 1-2-3 Kasumi, Minami-ku, Hiroshima 734-8553, Japan*

Received 6 December 2004; revised 13 July 2005; accepted 17 August 2005
Available online 20 October 2005

Abstract

Periodontal ligament (PDL) consists of different cell populations in various differentiation stages. In the present study, we isolated cell populations from rat molar PDL by sequential enzymatic digestion and characterized growth potential and mineralization activity of the PDL subpopulations (PDL-SP) to throw light on the mechanism of PDL remodeling and, in its turn, periodontal tissue regeneration. PDL attached to extracted rat molars was digested 2 mg/ml collagenase and 0.25% trypsin at 37°C for 30 min. Then four consecutive digestions were performed for 20 min each in a fresh digestive solution. The solutions were centrifuged to collect released cells and 5 PDL subpopulations (30M-, 50M-, 70M-, 90M-and 110M-PDL-SP) were obtained. Light microscopic observation showed that about a half of PDL in width attached on the root surface of extracted teeth and 30M-PDL-SP was considered to contain cells mainly from middle portion of PDL. Scanning electron microscopic examination indicated that 110M-PDL-SP was enriched by root lining cementoblastic cells. 30M-PDL-SP showed a high level of proliferative activity. Although the growth potential of a subpopulation decreased in PDL-SP toward the root surface, 110M-PDL-SP had a high proliferative activity equivalent to that of 30M-PDL-SP. Analyses of alkaline phosphatase (ALP) and mineralization activities showed that higher activities in PDL-SP toward the surface of roots and that 110M-PDL-SP had the highest activity of ALP and the largest number of mineralization nodules. The present study shows as supposed by previous studies on cell kinetics in PDL that subpopulations with larger growth potential were generally located in the middle portion of PDL and those with higher mineralization activities toward the surface of the roots. It is suggested, however, that a possible pathway of PDL cell turnover may exist within the PDL-SP on the root surface in addition to the generally recognized pathway from the middle area of PDL to root surface.

Keywords: Periodontal ligament; Proliferation; Mineralization; Sequential enzymatic digestion

Introduction

Periodontal ligament (PDL), a thin connective tissue between root cementum and alveolar bone, plays important roles such as supportive, sensory, nutritive and homeostatic functions [1,2]. Recent studies showed, furthermore, that the formative function of PDL is indispensable to consider regenerative periodontal therapies [1,2].

It has been reported that PDL cells have osteoblastic characters, such as expressing high activity of alkaline phosphatase (ALP) [3,4], synthesizing cAMP at the stimulation of parathyroid hormone [5], producing mineralized nodules in vitro in the presence of ascorbic acid (50 μg/ml), dexanethasone (5 μM) and β-glycerophosphate (10 mM) [6], and producing non-collagenous proteins such as osteopontin (OPN), osteocalcin (OCN), and bone sialoprotein (BSP) [6,7]. In these studies, however, PDL was examined as a tissue unit and PDL-derived cells were characterized in the lump.

* Corresponding author. Fax: +81 82 257 5619.
E-mail addresses: mmiya@hiroshima-u.ac.jp (M. Miyauchi), mhiraoka@hiroshima-u.ac.jp (M. Kitagawa), shiba@hiroshima-u.ac.jp (H. Shiba), hkuri@hiroshima-u.ac.jp (H. Kurihara), ttakata@hiroshima-u.ac.jp (T. Takata).

8756-3282/$ - see front matter © 2005 Elsevier Inc. All rights reserved.
doi:10.1016/j.bone.2005.08.021

McCulloch et al. [8,9] reported that progenitor cells in marrow spaces migrate into PDL by way of vascular channels and locate perivascularly. The progenitor cells then provide daughter cells that migrate to the bone and cementum surfaces and differentiate into cementoblasts or osteoblasts. Perivascular cells also considered to be the source of PDL fibroblasts. These findings suggest that PDL consists of different cell populations in various differentiation stages according to the position in PDL.

Sequential enzymatic digestion has been applied to obtain the different cell populations from bone tissue. Wong and Cohn obtained 6 subpopulations of bone cells by sequential digestion of mouse calvaria with collagenase and trypsin [10]. They showed that bone contains at least two types of target cells with different response to parathormone and calcitonin. Rao et al. also showed that cell populations obtained from rat calvaria by the same method had different response to parathyroid hormone or prostaglandin E1 [11]. Using enzymatic digestion, PDL cells obtained from tissues adherent to the extracted root surface in some studies and cellular characteristics of the cells were studied [12,13]. As mentioned above, however, the cells were harvested in the lump and analyzed as a tissue unit in those studies. D'Errico et al. [12] isolated a heterogeneous primary cell population of PDL cells from extracted root surface using 2-hour-enzymatic digestion, and demonstrated that root lining cells (cementoblasts) expressing OPN, OCN and BSP were included within the isolated PDL cells. So we considered that different PDL subpopulations (PDL-SPs) in various differentiation stages including PDL-SP enriched with cementoblasts located on root surface may be successfully isolated by sequential enzymatic digestion. The isolated PDL-SPs may be useful to determine regulation of the mechanisms of differentiation and proliferation of PDL and cementoblasts. Moreover they may be useful tool to establish the in vitro cell system.

In the present study, therefore, we reported the isolation of cell populations from rat molar PDL by sequential enzymatic digestion and characterized the growth potential and mineralization activity of PDL-SPs to throw light on the mechanism of remodeling of PDL.

Materials and methods

Isolation of PDL subpopulations and cell culture

The protocol of the studies was approved by the experimentation committee of the Faculty of Dentistry, Hiroshima University. After sacrificing by an overdose of chloroform, 100 molars were extracted from 10 Lewis male rats (8-week old, 220–250 g). To avoid contamination of gingival tissues, supracrestal soft tissues attached to the cervical area of the molars were carefully curretaged before the extraction. The extracted molars with PDL were rinsed once in Dulbecco's phosphate-buffered saline without calcium and magnesium (PBS, NISSUI PHARMACEUTICAL CO., LTD., Tokyo, Japan). Then, they were immersed in a digestion solution, 20 mL of Dulbecco's Modified Eagle Medium (DMEM) (Gibco BRL, N.Y, USA) containing 2 mg/mL collagenase (Wako, Tokyo, Japan) and 0.25% trypsin (DIFCO LABORATORIES, MI, USA), at 37°C for 30 min [12,13]. After that, four consecutive digestions were performed for 20 min each in a fresh solution. The solutions were centrifuged to collect released PDL cells. In this way, 5 PDL-SPs were obtained and named 30M-, 50M-, 70M-, 90M-and 110M-PDL-SP, respectively. The cells in each subpopulations were then cultured in DMEM with 10% fetal bovine serum (FBS) plus penicillin G sodium (10 unites/mL) and streptomycin sulfate (10 mg/mL) in a humidified atmosphere of 5% CO_2 at 37°C. The culture medium was changed once three days and cells at the third to fifth passages were used in following studies.

Light microscopic observation

To examine the amount of PDL attached to the root surface of extracted molars and the effect of sequential enzymatic digestion of the PDL, light microscopic observations with conventional and phase contrast microscopes were performed on some extracted teeth before and after the enzymatic digestion. For hematoxylin and eosin sections, the teeth were fixed in a 10% formaldehyde neutral buffer solution overnight, decalcified in a 10% EDTA solution (pH 7.4) for 2 weeks at 4°C and cut into paraffin embedded 4.5-micrometer section routinely.

Scanning electron microscopic observation

To observe the surface condition of digested PDL and root surface, each 3 teeth were prepared for scanning electron microscopy (SEM) at each digestion period. After gentle wash with PBS, the teeth were fixed in a 0.1 M cacodylate-buffered 2% paraformaldehyde and 2.5% glutaraldehyde solution (pH 7.4, 4°C) for 1 hour. The teeth were then post-fixed in a 0.1 M cacodylate-buffered 1% OsO4 solution (pH 7.4, 4°C) for 1 hour. They were dehydrated in a graded series of ethanol, critical-point-dried, and sputter-coated with gold-palladium. The specimens were examined in a JSM-6300 scanning electron microscope (Japan Electron Co., Tokyo) at 60 kv.

Cell growth analysis of PDL subpopulations

PDL cells of the subpopulations were plated in 24 well culture-plates at an initial density of 5×10^3 cells per well and cultured in DMEM containing 10% FBS, penicillin G sodium (10 unites/mL) and streptomycin sulfate (10 mg/mL). At day 2, 4 and 8, the cells were harvested, in triplicate wells, by incubating in 0.05% trypsin and 0.01% EDTA, and cell number were determined by Coulter counter Z1 (Coulter Electronic Ltd., UK). Morphology of the cultured PDL cells was observed by a phase-contrast microscope.

ALP-Activity of PDL subpopulations

ALP activity was assayed by biochemical methods. Cells of each PDL-SP were plated in 24 well culture plates (5×10^4 cells per well) and cultured in DMEM containing 10% FBS, penicillin G sodium (10 unites/mL) and streptomycin sulfate (10 mg/mL) for one week.

The quantitative analysis of ALP activity was performed by Bessey-Lowry enzymologic method using nitrophenyl phosphate as a substrate [14]. The cells were washed with PBS and homogenized ultrasonically in 0.5 mL of 10 mM Tris-HCl buffer (pH 7.4) containing 25 mM $MgCl_2$. Aliquots of the homogenates were used for determination of ALP activity and DNA content. One unite of ALP was defined as the amount of enzyme required to hydrolyze 1 nM *p*-nitrophenol per minute. DNA content was determined using bisbenzimidazole (Wako, Osaka, Japan) and ALP activities of PDL-SPs were expressed by unites per DNA contents.

Mineralization of PDL Cells

Mineralized nodule formation was examined by Dahl's stain for calcium [15]. Cells of PDL-SP were plated in 24 well-culture plates at a density of 5×10^4 cells per well and cultured in DMEM supplemented with 10% FBS, 50 μg/mL ascorbic acid, 10 mM sodium β-glycerophosphate and 10 nM dexamethasone for 3 weeks. Then the cells were fixed in a 10% formaldehyde neutral buffer solution and stained with alizarin red S. To clarify the nature of mineralized nodules, immunostaining for bone sialoprotein (BSP) was done. After blocking nonspecific staining with 0.5% casein for 20 min at RT, a rabbit polyclonal anti-BSP antibody (AB1854; CHEMICON, CA) was applied to 2% formaldehyde fixed cells at dilution of 1:500. Immunostaining was carried out using Dako-LSB2 kit (Dako, CA). The color developed with 0.025% 3,3′-diaminobenzidine

Table 1
Oligonucleotide primer sequences utilized in the RT-PCR

RT-PCR primer set		Sequence	Product length (bp)
COLI	F	5′-ctgaccttcctgcgcctgatgtcc-3′	300
	R	5′-gtctggggcaccaacgtccaaggg-3′	
ALP	F	5′-aggcaggattgaccacgg-3′	440
	R	5′-tgtagttctgctcatgga-3′	
OPN	F	5′-tccaaggagtataagcagcgggcca-3′	200
	R	5′-ctcttagggtctaggactagcttct-3′	
OCN	F	5′-cagccccctacccagat-3′	232
	R	5′-gaaagtatggacggcaca-3′	
BSP	F	5′-cactcacttgctctctccag-3′	385
	R	5′-ctgagagtgtggcgttgtgt-3′	
GAPDH	F	5′-tccaccaccctgttgctgta-3′	450
	R	5′-accacagtccatgccatcac-3′	

tetrahydrochloride in TRIS-HCL buffer plus hydrogenperoxide (Kyowa Medics, Tokyo). The cells were counterstained with Mayer's hematoxylin, dehydrated and then mounted.

Statistical analysis

Enumeration assay of triplicate wells was repeated 3 times. Total 9 wells were assayed in each experimental group. The results of cell growth analysis and quantitative analysis of ALP activity were shown as mean ± SE. The mean values obtained were analyzed for statistical differences using a nonparametric Mann-Whitney U-test. Probabilities less than 0.05 were considered as significant.

RNA preparation and reverse transcription-polymerase chain reaction analysis (RT-PCR)

Total RNA was isolated from cultures of confluent 30M-and 110M-PDL-SP cells using the RNeasy Mini Kit (Qiagen K.K., Tokyo, Japan) according to the manufacture's instructions. Preparations were quantified and their purity was determined by standard spectrophometric methods. cDNA was synthesized from 1 μg of total RNA according to the ReverTra Dash (Toyobo Biochemicals, Tokyo, Japan). The oligonucleotide RT-PCR primers for type I collagen (COLI), ALP, osteopontin (OPN), osteocalcin (OCN), BSP and glyceraldehydes-3-phosohate (GAPDH) listed in Table 1 were purchased from Invitrogen (Tokyo, Japan). Aliquots of total cDNA were amplified with 1.25 U of rTaq-DNA polymerase (Qiagen K.K.), and amplifications were performed in a PC701 thermal cycler (Astec, Fukuoka, Japan) for 32 cycles after an initial 30 sec denaturation at 94°C, annealed for 30 sec at 56°C, and extended for 1 min at 72°C in all primers. The amplification reaction products were resolved on 1.5% agarose/TAE gels (Katayama Chemical), electrophoresed at 100 mV, and visualized by ethidium-bromide staining.

Immunohistochemistry for BrdU incorporated and proliferating cell nuclear antigen (PCNA) in vivo rat PDL

To evaluate of cell proliferative activity in vivo PDL tissue, immunohistochemistry for BrdU and PCNA was done. Male 8-week-old Lewis rats were sacrificed by over dose of ethyl ether. At 2 hr before sacrifice, all rats ($n = 3$) were given a single intraperitoneal injection of BrdU (Sigma, St Louis) at a dosage of 100mg/kg body weight. Tissue samples were resected en block from molar region and fixed in a 10% formaldehyde neutral buffer solution overnight, decalcified in a 10% EDTA solution (pH 7.4) for 2 weeks at 4°C and cut into paraffin embedded 4.5-micrometer section routinely. The deparaffinizerd sections were incubated by 0.3% hydrogen peroxide in methanol to block the endogenous peroxidase activity for 30 min at room temperature (RT). For PCNA IHC, sections were placed in 0.01M citrate buffer (pH 6.0) for 15 min in a microwave oven. For BrdU-IHC, the sections were rinsed in tripsin buffer and then incubated with 95% formamide in 0.15M sodium citrate at 70°C for 45 min for denaturalization of DNA. After blocking nonspecific staining with 0.5% casein for 20 min at RT, mouse monoclonal anti-BrdU antibody (Bu20a; DAKO) and mouse monoclonal anti-PCNA antibody (PC-10; DAKO) were applied to the specimens at dilution of 1:100. Immunostaining was carried out using LSB2 kit as described above.

Results

Light microscopic findings of PDL on extracted molar roots

PDL attached to the root surface of extracted teeth was not completely uniform in thickness. However compared to the width of normal PDL (Fig. 1a), about a half of PDL in width was on an average seen on the root surface as shown in Fig. 1b. The width of PDL decreased with the enzymatic digestion and no cells were seen on the surface of teeth after digestion for 110 min (Figs. 1c, 2a–c). There were no findings suggesting release of pulpal cells from a pulp chamber due to the enzymatic digestion even in the specimens at 110 min digestion (Fig. 1c). The finding was indicative that contamination of pulpal cells into each PDL-SP was not evident.

Scanning electron microscopic findings

Roots of the extracted teeth were covered by rough collagenous PDL tissues and exposure of cementum was not seen (Fig. 2d). With time of digestion, the surface of PDL became smoother (Figs. 2e–h). Although a few cells were seen on the root surface after 90 min digestion (Fig. 2h), no cells were remained on the root surface and cementum was completely exposed at 110 min digestion (Fig. 2i). This result indicated that the 110M-PDL-SP was enriched by root lining cells.

Proliferation of PDL subpopulations

Cultured PDL cells were spindle in shape (Fig. 3a) and there was no obvious morphological difference among culture cells of PDL-SPs except 100M-PDL-SP, which consisted of more polygonal cells (Fig. 3b). Fig. 4a shows the proliferation curve

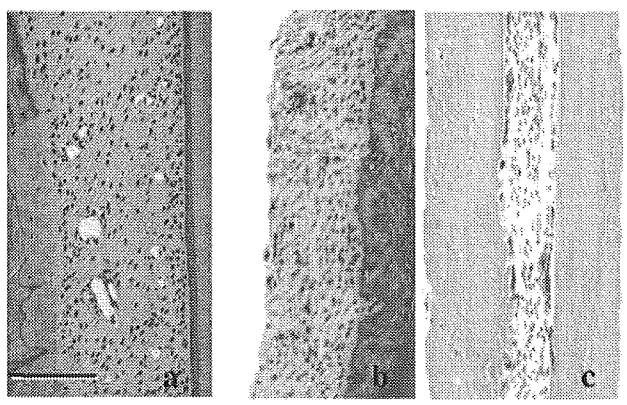

Fig. 1. Light microscopic features of PDL; normal PDL (a), before enzymatic digestion (b), and after 110 min digestion (c). About a half of PDL in width was seen on the root surface (b) compared to the normal PDL (a). No cells were seen on the root surface after digestion for 110 min (c). a–c: ×100, scale bar = 100 μm.

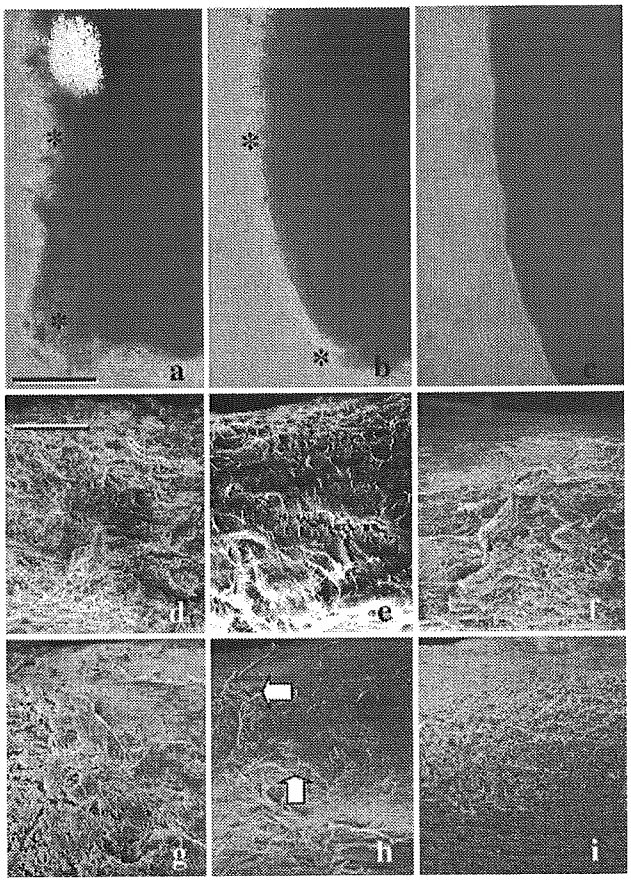

Fig. 2. Phase contrast microscopic features of PDL (*) before enzymatic digestion (a), after 70 min (b) and 110 min (c). The width of PDL decreases with the enzymatic digestion. No cells on the denuded root surface after 110 min digestion (c). a–c: ×100, scale bars = 100 μm. Scanning electron microscopic findings of periodontal ligament before digestion (d), after digestion for 30 min (e), 50 min (f), 70 min (g), 90 min (h) and 110 min (i). A few cells on the root surface (→) after 90 min digestion (h) are not seen after 110 min digestion (i). d–i: ×50, scale bar = 200μm.

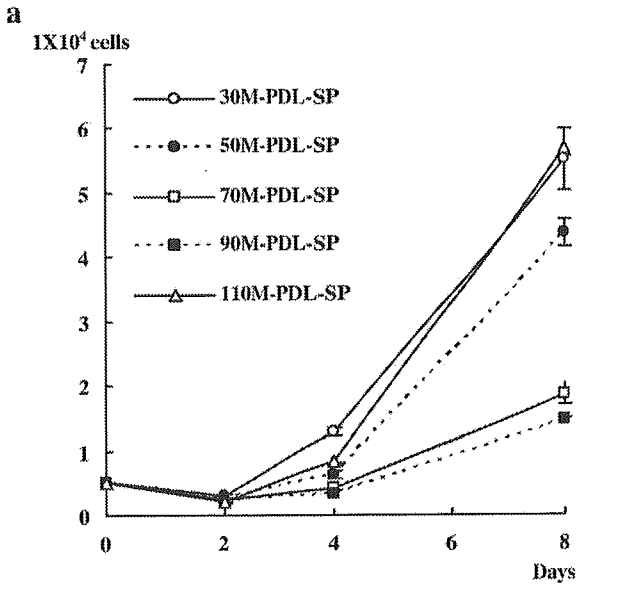

b

	50M PDL-SP	70M PDL-SP	90M PDL-SP	110M PDL-SP	Mixed PDL
30M-PDL-SP	*	*	*	-	-
50M-PDL-SP		*	*	*	*
70M-PDL-SP			*	*	*
90M-PDL-SP				*	*

* indicates significant difference (P<0.01)., indicates no significant difference between cell number of each group at day 8

Fig. 4. Proliferation potential of periodontal ligament subpopulations (PDL-SPs) (a) and significant differences between each PDL-SP (b). 30M-PDL-SP shows a high level of a proliferative activity. Proliferative activity of PDL-SP decreases toward the root surface, 110M-PDL-SP, however, has high proliferative potential equivalent to that of 30M-PDL-SP (Mann-Whitney U-test: $P < 0.001$ versus 50-, 70-, 90-PDL-SP).

of each PDL-SP and Fig. 4b lists significant differences ($P < 0.05$) between each PDL-SP. 30M-PDL-SP, which was enriched by cells from middle portion of PDL, showed a high level of a proliferative activity. Although the proliferative activity of PDL-SP decreased toward the root surface, 110M-PDL-SP, which was enriched by cells on the root surface, had high proliferative potential equivalent to that of 30M-PDL-SP.

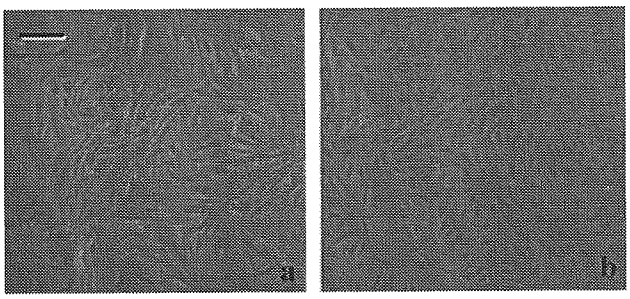

Fig. 3. Phase contrast microscopic features of 30M-PDL-SP (a) and 100M-PDL-SP (b). 30M-PDL-SP consists elongated spindle fibroblastic cells. In the culture cells of 110M-PDL-SP, a lot of more polygonal small cells (cementoblastic cell) were seen. a,b; ×150, scale bar = 33 μm.

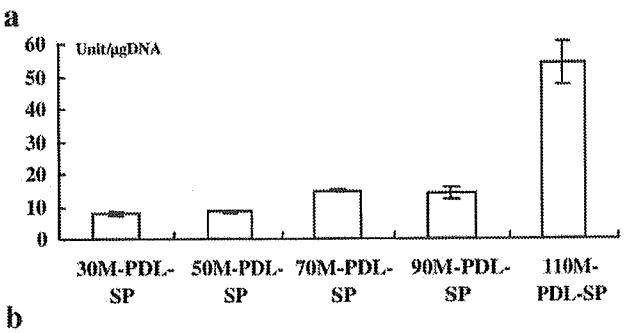

b

	50M PDL-SP	70M PDL-SP	90M PDL-SP	110M PDL-SP
30M-PDL-SP	n.s.	*	*	*
50M-PDL-SP		*	*	*
70M-PDL-SP			n.s.	*
90M-PDL-SP				*

n.s. = not significant; * = P<0.001.

Fig. 5. Quantitative measurement of alkaline phosphatase (ALP) activities (a) of periodontal ligament subpopulations (PDL-SPs) and significant differences between each PDL-SP (b).

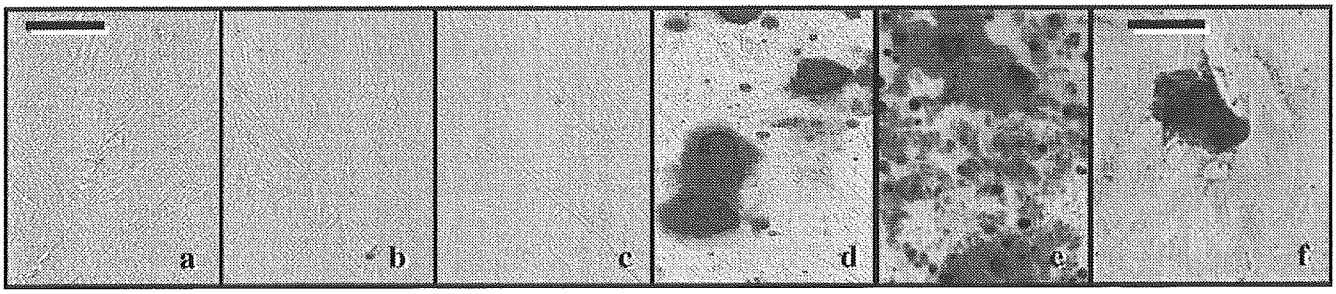

Fig. 6. Mineralization in periodontal ligament subpopulations (PDL-SPs). (a) 30M-PDL-SP, (b) 50M-PDL-SP, (c) 70M-PDL-SP, (d) 90M-PDL-SP, (e) 110M-PDL-SP. The most intensive staining is observed in 110M-PDL-SP and less in 90M-PDL-SP. a–e: ×150, scale bar = 33 μm. Immunoexpression of BSP in 110M-PSL-SP (f). Mineralized nodule is positively stained for BSP. h: ×300, scale bar = 16 μm.

ALP Activities of PDL subpopulations

The highest ALP activity was also shown by the quantitative analysis of the enzyme (Fig. 5a) and Fig. 5b shows significant differences between each PDL-SP. As a PDL-SP was derived from farther from the root surface, ALP activity of the subpopulation became less.

Mineralization

Well corresponding to the result of ALP activity, different amount of mineralization was seen among the PDL-SPs (Figs. 6a–e). Little or no staining was seen in 30M-, 50M-and 70M-PDL-SPs (Figs. 6a–c). The most intensive staining was observed in 110M-PDL-SP (Fig. 6e) and less in 90M-PDL-SP (Fig. 6d). BSP was immunohistochemically expressed in mineralized nodules and surrounding cells (Fig. 6f).

Expression of mRNA for mineralization related markers in 30M- and 110M-PDL-SPs

Although expression of COLI, ALP, OPN and OCN-mRNA was observed in both of 30M-and 110M-PDL-SPs, 110M-PDL-SP expressed higher levels of OPN and OCN-mRNA. In addition, BSP mRNA could be detected only in 110M-PDL-SP (Fig. 7).

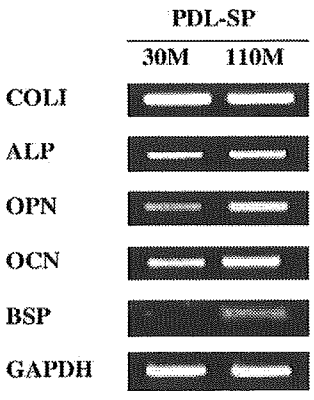

Fig. 7. mRNA-expression of mineralization related markers in 30M- and 110M-PDL-SPs. Expression of COLI, ALP, OPN and OCN mRNA was seen in both of 30M- and 110M-PDL-SPs. BSP-mRNA was only detected in 110M-PDL-SP.

Immunolocalization of PCNA and BrdU in vivo PDL

To confirm the high growth potential of 100M-SP-PDL, immunodetection of PCNA in vivo PDL (Fig. 8a) and BrdU incorporation into PDL cells (Fig. 8b) were examined. Positive cells for both proliferation markers were observed near the root surface as well as in the perivascular area in the middle of PDL.

Discussion

Enzymatic release of PDL cells from extracted roots has been applied in some studies and cellular characteristics of the cells were studied [12,13,16]. In those studies, however, the cells were harvested in the lump and analyzed as a tissue unit. In other words, heterogeneity of PDL has not been examined using subpopulations isolated from PDL by sequential enzymatic digestion, which has been applied to characterize heterogeneous calvarial cell populations [10,11]. Based on previous reports [12,13,16] and our preliminary studies, we decided on a 110 min. digestion to release all cell layers of PDL from extracted roots. Complete release of PDL cells was confirmed at the light and electron microscopic levels. It was also verified histologically that pulpal cells were not released into the

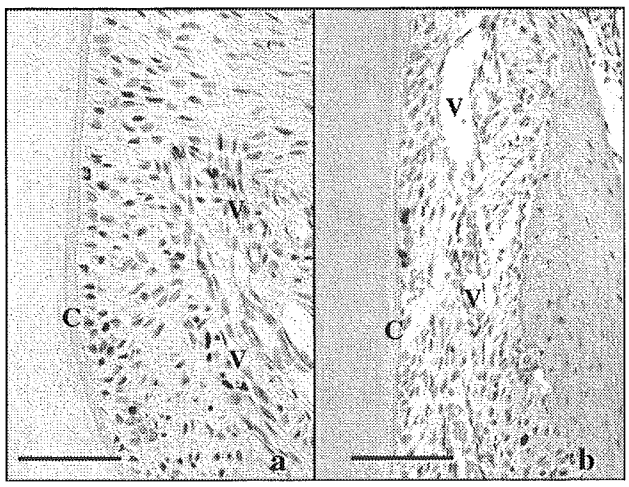

Fig. 8. Immunostaining for proliferating cell nuclear antigen in periodontal ligament (PDL) (a) and BrdU incorporation into PDL cells (b). Positive cells for both markers are observed in PDL cells near the root cementum (C) as well as in the perivascular area (V) in PDL. a: ×200, scale bar = 50 μm, b: ×100, scale bar = 100 μm.

digestions for the experimental period. In the present studies, we obtained 5 PDL-SPs. 30M-PDL-SP was considered to be isolated from the middle part of PDL, because about a half of the width of PDL attached to the extracted roots. Although light and electron microscopy showed a few layers of PDL cells on the root surface after 90 min digestion, those cells were completely disappeared from the root surface after 110 min digestion. Moreover, cementocytes located in mineralized cementum matrix were not released into the digestion without decalcification. We therefore regarded 110M-PDL-SP as a subpopulation enriched by lining cells on the root surface.

Studies on ALP and mineralization activities of the subpopulations showed that higher activities were seen in PDL-SP toward the root surface and that 110M-PDL-SP had by far the highest activity among the subpopulations. Groeneveld et al. [16,17] reported that high ALPase activity is observed in the area near cementum and alveolar bones at rat maxillary molar in vivo. Sasaki et al. [18] also showed that cementoblasts of human deciduous teeth exhibited intense ALP activity along the plasma membranes of whole cell surfaces. In addition, 110M-PDL-SP showed the expression of mineralization related genes, including COLI, ALP, OPN, OCN and BSP. Levels of OPN and OCN-mRNA in 110M-PDL-SP were higher than those in 30M-PDL-SP. BSP-mRNA could not be detected in 30M-PDL-SP. MacNeil et al. demonstrated that BSP, OPN and OCN mRNA were expressed selectively by cells lining the root surface (cementoblasts) during root development in mice. Our results and these findings also suggest that 110M-PDL-SP is enriched cells from the root surface: cementoblasts.

McCulloch et al. [8,9], based on their radioautographic studies of mouse mandibular molar prepared from animals pulse-injected with 3H-Tdr, reported that cells migrate from endosteal spaces into the PDL and they express the phenotypes for osteoblasts or cementoblasts. They showed that, numerous cells labeling with 3H-Tdr, which seemed to be progenitor cells, were observed in the surrounding blood vessel. Well corresponding to their results, 30M-PDL-SP obtained from the middle area of PDL showed a high proliferative potential and considered to be enriched progenitor cells.

PDL-SP gradually decreased its potential of growth as it approached toward the root surface. Interestingly, however, 110M-PDL-SP had a high proliferative activity equivalent to that of 30M-PDL-SP. To confirm the high growth potential of 110M-PDL-SP, immunodetection of proliferating cell nuclear antigen in PDL (Fig. 4a) and BrdU incorporation into PDL cells (Fig. 4b) were examined. Positive cells for both proliferation markers were observed near the root surface as well as in the perivascular area in the middle of PDL. Together with these findings, there are two possibilities that 110M-PDL-SP is a homogeneous cell population with high potentials of both mineralization and proliferation or heterogeneous population composed of cementoblasts with high potential of mineralization and immature cells with high growth potential which can differentiate into cementoblast. The latter is more likely, because cultured 110M-PDL-SP showed uneven staining pattern for ALP which was most intensive around mineralized nodules. The origin of the cells with such a high growth potential on root surface is not decided. During root formation, Hertowig's epithelial root sheath (HERS) disintegrates prior to cementogenesis and undifferentiated mesenchymal cells from dental follicle penetrate HERS to invade the root surface. The undifferentiated cells differentiate to cementoblasts at root surface and deposit initial cementum [19,20]. A potential explanation is that a part of the undifferentiated cells with high proliferative activity migrated from dental follicle took up residence near the root surface after the cementum formation period. Further studies is necessary to determine this unique cell population is existing only in PDL of the 8 week-old animals examined or lasting there to the end of their life. If such an interesting population exists ever since, the population might play great roles especially in periodontal tissue remodeling and regeneration.

Although we could not characterize PDL-SPs in alveolar bone half of PDL, the present studies showed 1. PDL-SPs obtained from the cementum half of PDL by sequential enzymatic digestion showed different activities in proliferation and mineralization. 2. PDL-SPs with higher proliferation rates were generally located in the middle portion of PDL and those with higher mineralization activities were seen toward the surface of the roots. 3. PDL-SP on the root surface showed high activities of proliferation and mineralization. It is suggested that a possible pathway of PDL cell turnover may exist within the PDL-SP on the root surface in addition to the generally recognized pathway from the middle area of PDL to root surface. To clarify the mechanism of cellular proliferation and differentiation in PDL using PDL-SPs will provide indispensable data for developing new regenerative periodontal therapies. There is a possibility that the implantation of isolated root lining cell population having the high potential both of proliferation and minertalization may bring the adequate formation of cementum, which is needed for regeneration of periodontal tissue lost due to the periodontal disease.

Acknowledgments

This work was supported in part by grants 10557159 and 11470378 from the Ministry of Education, Science, Sports and Culture, Japan.

References

[1] Freeman E. Periodontium. In: Ten Cate AR, editor. Oral histology: development, structure and function. St. Louis: Mosby; 1994. p. 276–312.
[2] Carranza FA, Ubios AM. The tooth-supporting structures. In: Carranza FA, Newman MG, editors. Clinical periodontology. Philadelphia: WB Saunders; 1996. p. 30–51.
[3] Giannopoulou C, Cimasoni G. Functional characteristics of gingival and periodontal ligament fibroblasts. J Dent Res 1996;75:895–902.
[4] Ogata Y, Niisato N, Sakurai T, Furuyama S, Sugiya H. Comarison of the characteristics of human gingival fibroblasts and periodontal ligament cells. J Periodontol 1995;66:1025–31.
[5] Somerman MJ, Young MF, Foster RA, Moehring JM, Imm G, Sauk JJ. Characteristics of human periodontal ligament cells in vitro. Arch Oral Biol 1990;35:241–7.
[6] Ramakrishnan PR, Lin WL, Sodek W-L, Cho M-Il. Synthesis of

noncollagenous extracellular matrix proteins during development of mineralized nodules by rat periodontal ligament cells in vitro. Calcif Tissue Int 1995;57:52–9.
[7] Noutcu RM, McCauley LK, Koh AJ, Somerman MJ. Expression of extracellular matrix proteins in human periodontal ligament cells during mineralization in vitro. J Periodontol 1997;68:320–7.
[8] McCulloch CAG, Melcher AH. Cell density and cell generation in the periodontal ligament of mice. Am J Anat 1983;167:43–58.
[9] McCulloch CAG, Nemeth E, Lowenberg B, Melcher AH. Paravascular cells in endosteal spaces of alveolar bone contribute to periodontal ligament cell population. Anat Rec 1987;219:233–42.
[10] Wong GL, Cohn DV. Target cells in bone for parathormone and calcitonin are different; Enrichment for each cell type by sequential digestion of mouse calvaria and selective adhesion to polymeric surface. Porc Natl Acad Sci U S A 1975;72:3167–71.
[11] Rao LG, NG B, Brunette DM, Heersche JNM. Parathyroid hormone-and prostaglandin E1-response in a selected population of bone cells after repeated subculture and storage at −80 C. Endocrinology 1977;100:1233–41.
[12] D'Errico JA, MacNeil RL, Takata T, Berry J, Strayhorn CL, Somerman MJ. Expression of bone associated markers by tooth root lining cells, in situ and in vitro. Bone 1997;20:117–26.
[13] MacNeil RL, D'Errico JA, Ouyang H, Berry J, Strayhorn C, Somerman MJ. Isolation of murine cementoblasts: unique cells or uniquely-positioned osteoblasts? Eur J Oral Sci 1998;106:350–6.
[14] Shiba H, Nakamura S, Shirakawa M, Nakanishi K, Okamoto H, Satakeda H, et al. Effects of basic fibroblast growth factor on proliferation, the expression of osteonectin (SPARK) and alkaline phosphatase, and calcification in cultures of human pulp cells. Dev Biol 1995;170:457–66.
[15] Vacca LL. Calcification. Laboratory manual of histochemistry. New York: Raven Press; 1985. p. 334–6.
[16] Groeneveld MC, Everts V, Beertsen W. Alkaline phosphatase activity in the periodontal ligament and gingival of the rat molar: Its relation to cementum formation. J Dent Res 1995;74:1374–81.
[17] Groeneveld MC, Everts V, Beertsen W. A quantitive enzyme histochemical analysis of the distribution of alkaline phosphatase activity in the periodontal ligament of the rat incisor. J Dent Res 1993;72:1344–50.
[18] Sasaki T, Watanabe C, Shimizu T, Debari K, Segawa K. Possible role of cementoblasts in the resorbant organ of human decidous teeth during root resorption. J Periodontal Res 1990;25:143–7.
[19] Cho MI, Grant PR. Ultrastructuarl evidence of directed migration during initial cementoblast differentiation in root formation. J Periodontal Res 1988;23:68–76.
[20] Diekwisch TG. The development biology of cementum. Int J Dev Biol 45 (21001):695–706.

Histochem Cell Biol (2005) 123: 275–281
DOI 10.1007/s00418-005-0773-6

ORIGINAL PAPER

**Eiji Tanaka · Junko Aoyama · Mutsumi Miyauchi
Takashi Takata · Koichi Hanaoka · Tatsunori Iwabe
Kazuo Tanne**

Vascular endothelial growth factor plays an important autocrine/paracrine role in the progression of osteoarthritis

Accepted: 13 January 2005 / Published online: 15 March 2005

Abstract Vascular endothelial growth factor (VEGF) plays an essential role in the angiogenesis of growing cartilage. Although VEGF expression in cartilage vanishes in normal adults, VEGF is known to be expressed in chondrocytes of osteoarthritic (OA) cartilage. As little information is available on the VEGF expression in the cartilage of OA-like lesions of the temporomandibular joint (TMJ), VEGF expression in the condylar cartilage of TMJs of rats affected with OA was examined. To evoke OA, mechanical stress was applied by forced jaw opening for 10 or 20 days. After 20 days, marked OA-like lesions were observed in the condyle. VEGF was expressed in the chondrocytes of the mature and hypertrophic cell layers of the intermediate and posterior region of the condyle. The percentage of VEGF immunopositive chondrocytes significantly increased with the period of applied mechanical stress. Furthermore, tartrate-resistant acid phosphatase (TRAP) staining of the condylar cartilage showed significant increment of osteoclasts in the mineralized layer subjacent to the hypertrophic layer where high VEGF expression could be detected. The results suggest that VEGF plays an important role in the progression of OA.

Eiji Tanaka and Junko Aoyama contributed equally to this work.

E. Tanaka (✉) · J. Aoyama · K. Hanaoka · T. Iwabe · K. Tanne
Department of Orthodontics and Craniofacial Developmental Biology, Hiroshima University Graduate School of Biomedical Sciences, 1-2-3 Kasumi, Minami-ku, 734-8553 Hiroshima, Japan
E-mail: etanaka@hiroshima-u.ac.jp
Tel.: +81-82-2575686
Fax: +81-82-2575687

M. Miyauchi · T. Takata
Department of Oral Maxillofacial Pathobiology, Hiroshima University Graduate School of Biomedical Sciences, 1-2-3 Kasumi, Minami-ku, 734-8553 Hiroshima, Japan

Introduction

Articular cartilage is an avascular tissue, which produces angiogenic inhibitors (Horner et al. 2001). The hypertrophic cartilage layer, however, acts as a target for capillary invasion and angiogenesis with synthesis of angiogenic activators (Descalzi et al. 1995; Alini et al. 1996). Angiogenesis is considered to be essential for replacement of cartilage by bone during skeletal growth and regeneration (Gerber et al. 1999). Vascular endothelial growth factor (VEGF) is a potent angiogenic peptide with specific mitogenic and chemotactic actions on endothelial cells (Garcia-Ramirez et al. 2000). VEGF is produced by the chondrocytes of the hypertrophic cartilage layer, and together with its receptors (Flt-1 and Flk-1), it plays an essential role in both embryonic vasculogenesis and angiogenesis during normal growth (Gerber et al. 1999; Horner et al. 1999; Pufe et al. 2001; Aoyama et al. 2004). Although these VEGF-induced processes discontinue after the growth period, the presence of VEGF most likely continues to be required for active angiogenesis in processes such as tissue remodeling and wound healing and may play a role in malignant or certain inflammatory diseases of the adult (Neufeld et al. 1999). VEGF is also produced in chondrocytes of cartilage in joints affected with osteoarthritis (OA) (Neufeld et al. 1999; Enomoto et al. 2003). VEGF could have a pivotal role in the formation of new vessels in OA cartilage (Radin and Paul 1971). Indeed, osteophyte formation and extension of the subchondral growth plate have been observed in OA. These processes are very similar to enchondral ossification, which is highly dependent on VEGF (Gerber et al. 1999).

In the temporomandibular joint (TMJ), OA can be caused by a variety of mechanical and/or inflammatory factors. Previous studies have demonstrated VEGF expression in affected TMJ discs. This expression correlates with formation of new vessels in the avascular portions of the disc as well as with the prevalence of

chondroblast- and fibroblast-like cells (Leonardi et al. 2003). Little information is, however, available on the expression of VEGF in the condylar cartilage of the osteoarthritic TMJ. We tested the following hypotheses: (1) OA-like lesions can be induced by repeated mechanical overloads in a time-dependent manner, and (2) the expression and localization of VEGF in the condylar cartilage can be associated with mechanical overloading.

Materials and methods

Experimental animals

Fifteen 9-week-old Wistar strain male rats were used in this investigation. They were fed a stock diet with water ad libitum. The animals were divided into three groups of five. In two experimental groups, the TMJ was repetitively overloaded during a period of, respectively, 10 or 20 days; the third group served as an untreated (control) group. All procedures performed in this experiment were approved by the Hiroshima University Animal Care and Use Committee.

Application of mechanical stress

In the experimental animals, mechanical stress was applied to both TMJs by applying extended mouth opening for 1 h/day by using a jaw-opening device. This device kept the mandible in a maximal mouth-opening position of 30 mm. During this period of joint overload, the rats were anesthetized with intraabdominal injections of sodium pentobarbital (Nembutal; Dinabott, Osaka, Japan) at a dose of 50 mg/kg body weight, This procedure was repeated for 10 or 20 consecutive days. In the control animals, no mouth opening was applied although the same anesthesia schedule was maintained.

Tissue preparation

After the experimental period, the animals were killed with an overdose of anesthesia. The animals of the control group were killed after 10 days. Both TMJs were resected and fixed in 10% buffered paraformaldehyde and decalcified with 10% EDTA for 4 weeks at 4°C. Thereafter, they were embedded in paraffin, and serial sections (7 μm) were cut in the sagittal plane. The sections were stained with hematoxylin and eosin (HE) for histological examination.

Immunohistochemistry

To investigate the expression of VEGF in the condylar cartilage, immunohistochemical staining was performed using an anti-VEGF antibody (Immuno Biological Laboratories, Fujioka, Japan). Immunostaining was carried out using a Histofine simple stain kit (Nichirei, Tokyo, Japan). Briefly, after blocking endogenous peroxidase activity with 0.3% hydrogen peroxide in methanol, nonspecific binding of the antibody was blocked by incubating the section for 30 min with nonspecific staining blocking reagent (Dako, Carpinteria, CA, USA). Thereafter, it was incubated with the VEGF antibody (20 μg/ml in PBS) at 4°C overnight in a humid atmosphere. After washing, the sections were incubated with goat antirabbit IgG (Fab-fragment) conjugated to peroxidase-labeled amino acid polymer for 45 min. Color was developed with 0.02% 3,3′-diaminobenzidine (DAB) and 0.006% H_2O_2 in 0.05 M Tris–HCl buffer (pH 7.6). The sections were then dehydrated, mounted, and counterstained with Mayer's hematoxylin. The localization of VEGF-positive cells in the condylar cartilage was microscopically examined. Staining specificity was ascertained by substitution of the primary antibody with PBS or 3% normal rabbit serum.

Tartrate-resistant acid phosphatase (TRAP) staining

Tartrate-resistant acid phosphatase (TRAP) activity was examined for characteristics of osteoclast lineage cells according to the method of Minkin (1982). The staining medium contained naphthol AS-MX phosphate (Sigma Chemical Co., St. Louis, MO, USA) as substrate, Fast red violet LB salt (Sigma) as the coupler, and 50 mM sodium tartrate (Wako, Osaka, Japan). Counterstaining was performed with hematoxylin. Negative staining was performed without substrate.

Histometric analysis

From each TMJ, we selected one section from the midsagittal plane of the condyle. The condylar cartilage in each section was divided into anterior, intermediate, and posterior regions, as they are anatomically and functionally distinct areas. Furthermore, in each region, the condylar cartilage was divided into four layers (fibrous layer, proliferating cell layer, mature cell layer, hypertrophic cell layer). In each of these 12 areas (three regions × four layers), the number of VEGF-positive and -negative chondrocytes was counted under a fixed measuring frame (450 μm × 900 μm); the percentage of VEGF-positive cells was calculated as the number of VEGF-positive cells per the total number of chondrocytes under a fixed measuring frame. All chondrocytes in which cytoplasm was distinctively stained were considered to be VEGF positive. Using one section with TRAP staining through the midsagittal plane of the condyle, the number of osteoclasts was also counted in the mineralized layer subjacent to the hypertrophic cell layer of condylar cartilage. TRAP-positive cells with two or more nuclei were counted as osteoclasts. For each animal, the mean of both TMJs was calculated. For each of

the three groups, mean ± SD values were determined. We used Scheffe's test to check for differences in the numbers of total cell, VEGF-positive cell, and TRAP-positive osteoclasts between the experimental and control animals. Probabilities of less than 0.05 were considered to be significant.

Results

Histological and immunohistochemical findings

The condyles from the control animals showed smooth articular surfaces without signs of OA (Fig. 1A, C). Their four different layers could easily be distinguished, and the cells were regularly arranged. In addition, the disc contained many cells, and its collagen fibers were running regularly (Fig. 1B); the disc showed no degenerative changes.

The condylar cartilage of the animals that had experienced joint overload for 10 days (the 10-day group) had a normal appearance, with the exception of one joint that showed an irregular cell alignment in the posterior region of the condyle (Fig. 1D–F). In the 20-day group, marked OA-like lesions were observed in the condylar cartilage (Fig. 1G–I), including decrease in the thickness of the cartilage layer, irregularities of chondrocyte alignment, compressive necrosis of chondrocytes, and hyalinization of cartilage matrix in the proliferating, mature, and hypertrophic cell layers. In addition, increase of blood vessel and multinucleated osteoclasts was observed in the area subjacent to the hypertrophic cell layer. These changes were mainly detected in the intermediate and posterior region of the condyle. Furthermore, the disc showed extensive degenerative alterations, such as thinning, hyalinization, and cell-free areas (Fig. 1H).

In the control group, very few VEGF-positive cells could be detected in any of the cartilage layers (Fig. 2A). In the 10-day group, VEGF was abundantly expressed in the chondrocytes located in the mature and hypertrophic cell layer of the intermediate and posterior region of the condyle (Fig. 2B). In the 20-day group, VEGF expression of chondrocytes in the mature and hypertrophic cell layers was enhanced with respect to the 10-day group (Fig. 2C). Chondrocytes near necrotic areas showed prominent VEGF expression.

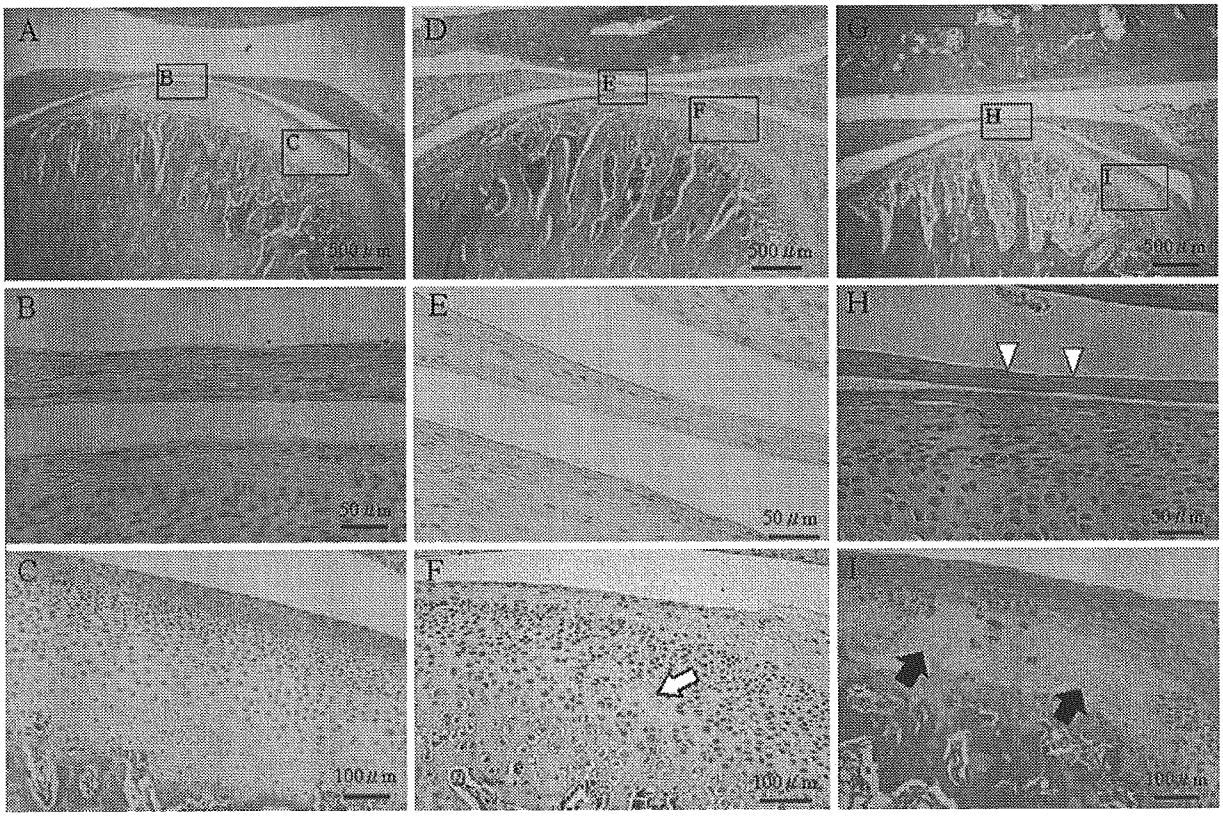

Fig. 1 Hematoxylin and eosin (HE)-stained sections of the rat temporomandibular joint (TMJ) after stress application. **A** Control TMJ. **B, C** Higher magnification of the area within the rectangular frame placed on *panel A*. **D** Experimental TMJ after 10 days' jaw opening. **E, F** Higher magnitude of the area within the rectangular frame placed on *panel D*. Condylar cartilage appeared to be normal except for one condyle with an irregular cell alignment in the posterior region (*white arrow, panel F*). **G** Experimental TMJ after 20 days' jaw opening. **H, I** Higher magnitude of the area within the rectangular frame placed on *panel G*. Osteoarthritis-like lesions were observed in the condylar cartilage. The articular disc showed thinning, hyalinization, and cell-free areas (*white arrowhead, panel H*). The condylar cartilage showed irregularities of chondrocyte alignment, pressure death of chondrocytes, and extensive hyalinization (*black arrow, panel I*)

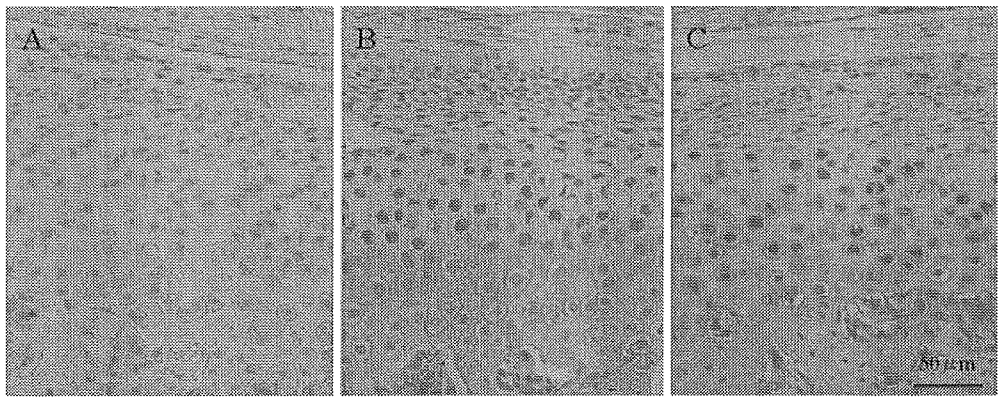

Fig. 2 Immunohistochemical staining of vascular endothelial growth factor (VEGF) in the condylar cartilage. **A** Control group. **B** Ten-day group. **C** Twenty-day group. VEGF-positive cells (*brown, panel B and C*) were detected only in the mature and hypertrophic cell layers

In the control group, small number of TRAP-positive osteoclasts was seen in the mineralized layer (Fig. 3A). Mechanical stress applied by forced jaw opening induced obvious increase in number of osteoclasts in the mineralized layer subjacent to mature and hypertrophic cell layers where VEGF expression was upregulated (Fig. 3B, C).

Histometric findings

Total cell number

In the control group, the total number of chondrocytes in the midsagittal section of the condylar cartilage was 191 ± 19, 208 ± 10, and 316 ± 28 (mean ± SD) at the anterior, intermediate, and posterior regions, respectively (Fig. 4). In all three regions, the proliferating cell layer contained the largest amount of chondrocytes. There were no significant differences in the number of chondrocytes between the control and experimental groups in the anterior region. In the intermediate and posterior region, the total number of chondrocytes was significantly smaller ($P < 0.05$) in the 20-day group than in the 10-day group. The difference in cell number was largest in the posterior region where the number of chondrocytes in the proliferating and mature cell layers was significantly less in the 20-day group ($P < 0.05$).

The number of VEGF-positive cells

The average amount of VEGF-positive cells in the cartilage of the condyle of the control group was 9.6%. This amount increased significantly ($P < 0.05$) to more than 40% in both experimental groups (Fig. 5). In the 10-day group, this increase was predominantly observed in the mature and hypertrophic cell layer, with a percentage of VEGF-positive cells of 79.1% and 79.5%, respectively; these percentages were significantly larger than those in the control group ($P < 0.05$). In the 20-day group, the increase of VEGF-positive cells compared with the

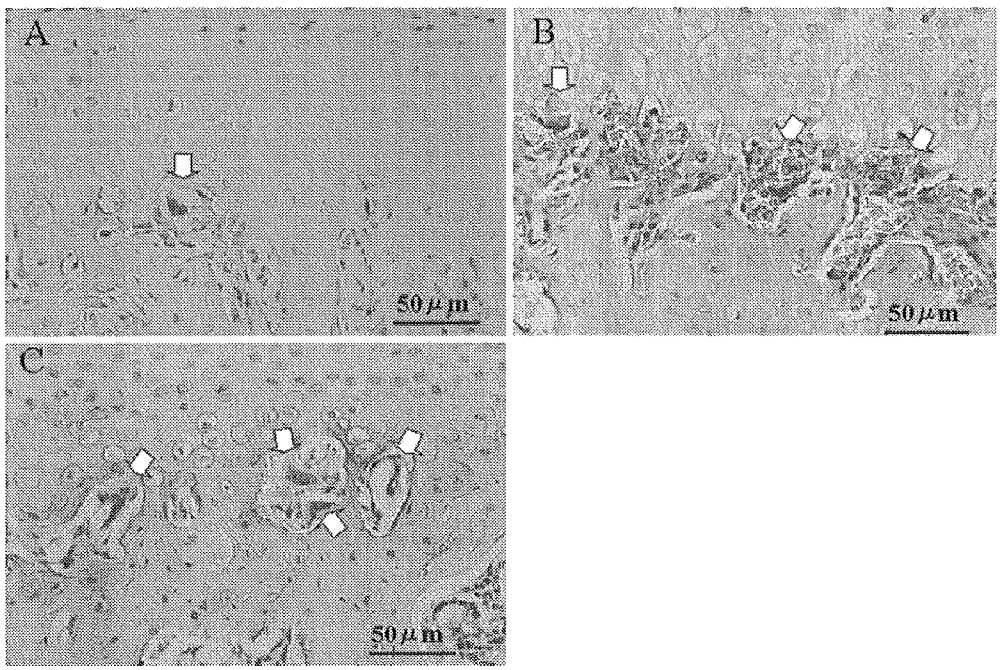

Fig. 3 Tartrate-resistant acid phosphatase (TRAP) staining in the mineralized layer subjacent to the hypertrophic cell layer of condylar cartilage. **A** Control group. **B** Ten-day group. **C** Twenty-day group. *White arrows* indicate osteoclasts

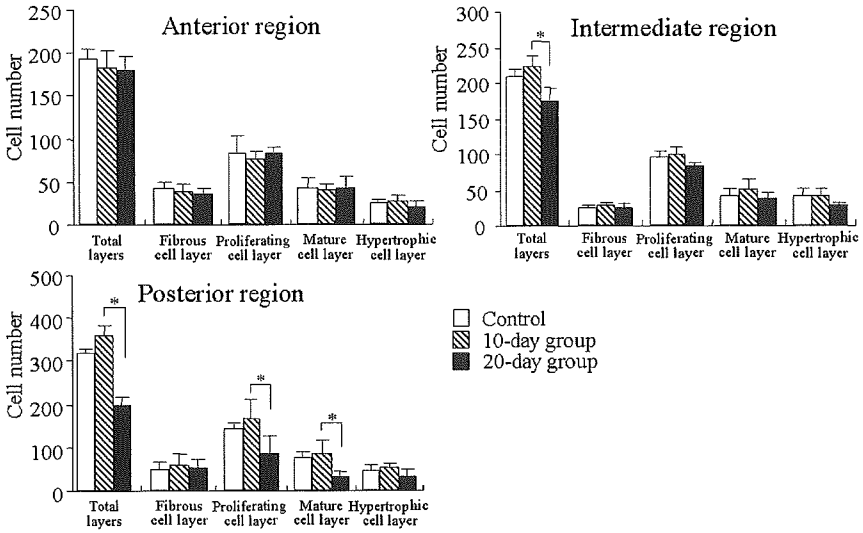

Fig. 4 Number of chondrocytes in the various regions and layers of the condylar cartilage. The *asterisk* indicates $P < 0.05$ using a Scheffe's test

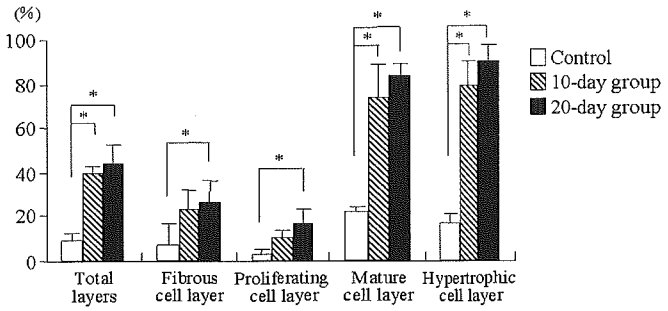

Fig. 5 Percentage of vascular endothelial growth factor (VEGF)-positive cells in the condylar cartilage. The *asterisk* indicates $P < 0.05$ using a Scheffe's test

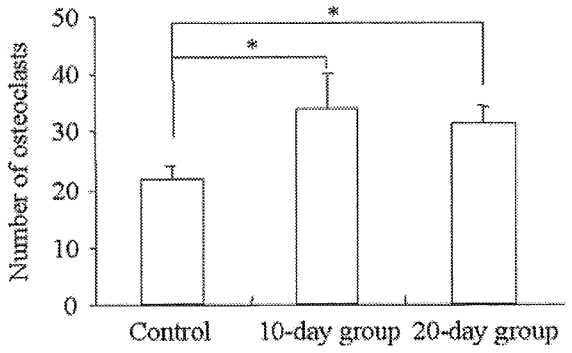

Fig. 6 Number of osteoclasts in the mineralized layer subjacent to the hypertrophic cell layer of condylar cartilage. The *asterisk* indicates $P < 0.05$ using a Scheffe's test

control group was significant ($P < 0.05$) in all cartilage layers.

The number of TRAP-positive osteoclasts

In the control group, the number of osteoclasts detected in the mineralized layer was 22.0 ± 2.0 (Fig. 6). After a forced mouth opening, the numbers of TRAP-positive osteoclasts were 34.0 ± 5.8 in the 10-day group and 31.5 ± 3.1 in the 20-day group. There were significant differences in the number of osteoclasts between the control and experimental groups ($P < 0.05$).

Discussion

In growing articular cartilage, hypertrophic chondrocytes promote vascularization in the hypertrophic cell layer in the growth plate by production of VEGF, but this process discontinues in the adult (Gerber et al. 1999). Furthermore, normal chondrocytes secrete antiangiogenic peptides and inhibitors of proteases. As these constituents are involved in extracellular matrix degradation (Moses et al. 1999), they must likely inhibit angiogenesis, which can explain why articular cartilage is normally an avascular tissue. Conversely, in OA cartilage, a focal premature differentiation of chondrocytes to hypertrophic cells was demonstrated (von der Mark et al. 1992). These hypertrophic cells produce VEGF, which may contribute to the inflammatory process in OA. It is likely that similar processes occur during the development of OA in the TMJ as a result of mechanical stress. However, in contrast to the many reports on the role of VEGF in inflammatory arthritis, such as rheumatoid arthritis, there are few reports on its role in OA in the TMJ, despite its frequent occurrence. The present study is, as far as we know, the first in which the VEGF expression in the condylar cartilage of TMJ-OA has been examined.

Unlike rheumatoid arthritis and synovitis, TMJ-OA has primarily a noninflammatory origin (Zarb and Carlsson 1995). The pathological process is characterized by deterioration and abrasion of articular cartilage and local thickening and remodeling of the underlying bone (Zarb and Carlsson 1995). These changes are frequently accompanied by the superimposition of secondary inflammatory changes. Therefore, mechanically induced OA may better reflect TMJ-OA. Recently,

Fujisawa et al. (2003) reported on the possibility of developing OA-like lesions in the rabbit TMJ by forced mouth opening. Their experimental protocol included a repetitive, steady, mouth opening of 3 h/day for 5 days. Muto et al. (1995) investigated pathological changes of the rat TMJ induced by repeated mouth opening of 20 mm ten times per day for 10 days. Although these authors reported the occurrence of synovitis and fibrous adhesions, it would not be appropriate to call these findings OA. Considering these findings, we used a protocol of a forced mouth opening of 30 mm for 1 h/day. With this protocol, OA-like lesions in the TMJ could be induced that were similar to those observed in TMJ-OA patients. After 20 days of forced mouth opening, marked OA-like lesions could be recognized. Therefore, our protocol of forced mouth opening can be considered as a useful model to evaluate the initiation and advancement of OA.

The VEGF expression in OA cartilage appeared to be progressive with the applied mechanical overload. Freemont et al. (1997) reported that VEGF expression in chondrocytes is induced by high-intensity stress and acts in cartilage as an autocrine inducer of matrix metalloproteinases (MMPs). Furthermore, Forsythe et al. (1996) reported that VEGF induction in chondrocytes by mechanical overload is linked to activation of the hypoxia-induced transcription factor-1 (HIF-1), which is known to bind to hypoxia response element (HRE) in the human VEGF gene promoter. Pufe et al. (2004) also reported that after mechanical overload chondrocytes were strongly immunopositive for HIF-1, resulting in induction of VEGF. Consequently, mechanical overload induces HIF-1, and the subsequently generated VEGF activates the chondrocytes autocrinally for producing MMP-1, -3, and -13. Tissue inhibitors of metalloproteinase (TIMP-1 and -2) are then reduced by mechanical overload (Pufe et al. 2004). These findings indicate that VEGF is probably induced in chondrocytes by mechanical overload, probably facilitating hypoxia to mediate the destructive processes associated with OA as an autocrine factor. It must be noted that the presence of hypoxia and its association with VEGF was not the subject of the present study.

Furthermore, we observed that the number of blood vessels and osteoclasts obviously increased in the area subjacent to the hypertrophic cell layer where a number of VEGF-expressing chondrocytes could be detected after a forced jaw opening. It is reported that VEGF played an important role not only in endothelial cell recruitment but also in osteoclast recruitment (Niida et al. 1999; Engsig et al. 2000). Niida et al. (1999) demonstrated that M-CSF and VEGF have overlapping functions in the support of osteoclastic bone resorption. These findings suggested that VEGF produced by chondrocytes might be responsible for migration into cartilage, differentiation, and stimulation of preosteoclasts and osteoclasts. Then, the increase of osteoclasts stimulated by VEGF may induce destruction of cartilage and make vascular invasion into the condylar cartilage easier.

Chondrocyte maturation is considered to be arrested in normal, healthy, articular cartilage whereas at the onset of OA, this arrest may be discontinued. Wong et al. (2003) examined the effect of cyclic tension and cyclic hydrostatic pressure on the expression of VEGF, MMP-13, and TIMP-1 in cultured chondrocytes and showed that VEGF was significantly upregulated by both cyclic tension and hydrostatic pressure. Cyclic hydrostatic pressure downregulated the expression of MMP-13 and upregulated expression of TIMP-1 while cyclic tension upregulated MMP-13 and downregulated TIMP-1. This implies that chondrocyte differentiation is slowed by cyclic hydrostatic pressure and accelerated by cyclic tension. Ohashi et al. (2002) investigated the effects of different magnitudes of dynamic loading on growth plate biology and showed that cartilage mineralization was suppressed and VEGF expression in chondrocytes was accelerated proportionally with the magnitude of applied force. Considering these findings, chondrocytes, especially hypertrophic chondrocytes, appear to have evolved complex mechanoresponsive mechanisms.

In the present study, we found that in both the experimental groups, VEGF was detected in more than 80% of the chondrocytes of the mature and hypertrophic cell layer. The 10-day group showed an increase in the number of cartilage cells without marked pathological changes in the TMJ while the 20-day group showed obvious pathological changes of the articular cartilage and disc with a decrease in number of cartilage cells and a percentual increase of VEGF immunoreactive cells. Judging from our results, chondrocyte maturation also depends on the rate and period of mechanical overloading.

In conclusion, VEGF was expressed by articular chondrocytes (especially in the hypertrophic cell layer) in the mandibular condyle after mechanical overloads by a forced mouth opening. The percentage of VEGF immunopositive chondrocytes increased significantly with the period of forced mouth opening. It is suggested that VEGF plays an important autocrine or paracrine role in the initiation and progression of OA in the TMJ.

References

Alini M, Marriott A, Chen T, Abe S, Poole AR (1996) A novel angiogenic molecule produced at the time of chondrocyte hypertrophy during endochondral bone formation. Dev Biol 176:124–132

Aoyama J, Tanaka E, Miyauchi M, Takata T, Hanaoka K, Hattori Y, Sasaki A, Watanabe M, Tanne K (2004) Immunolocalization of vascular endothelial growth factor in rat condylar cartilage during postnatal development. Histochem Cell Biol 122:35–40

Descalzi Cancedda F, Melchiori A, Benelli R, Gentili C, Masiello L, Campanile G, Cancedda R, Albini A (1995) Production of angiogenesis inhibitors and stimulators is modulated by cultured growth plate chondrocytes during in vitro differentiation: dependence on extracellular matrix assembly. Eur J Cell Biol 66:60–68